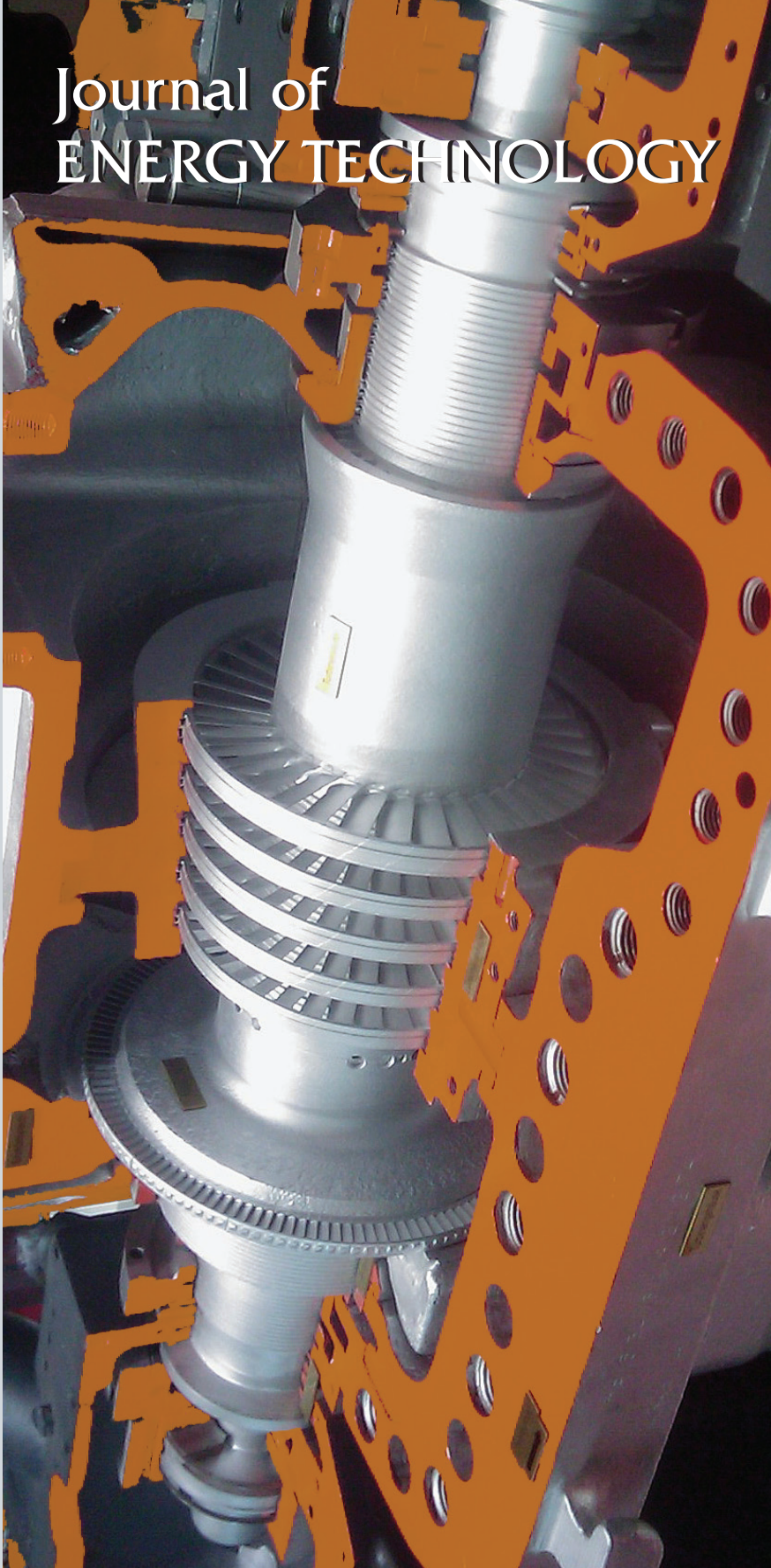




Faculty of Energy Technology

# Journal of ENERGY TECHNOLOGY



Volume 7 / Issue 3

AUGUST 2014

[www.fe.um.si/en/jet.html](http://www.fe.um.si/en/jet.html)



# Journal of ENERGY TECHNOLOGY



## **VOLUME 7 / Issue 3**

Revija Journal of Energy Technology (JET) je indeksirana v naslednjih bazah: INSPEC®, Cambridge Scientific Abstracts: Abstracts in New Technologies and Engineering (CSA ANTE), ProQuest's Technology Research Database.

The Journal of Energy Technology (JET) is indexed and abstracted in the following databases: INSPEC®, Cambridge Scientific Abstracts: Abstracts in New Technologies and Engineering (CSA ANTE), ProQuest's Technology Research Database.



# JOURNAL OF ENERGY TECHNOLOGY

## Ustanovitelj / FOUNDER

Fakulteta za energetiko, UNIVERZA V MARIBORU /  
FACULTY OF ENERGY TECHNOLOGY, UNIVERSITY OF MARIBOR

## Izdajatelj / PUBLISHER

Fakulteta za energetiko, UNIVERZA V MARIBORU /  
FACULTY OF ENERGY TECHNOLOGY, UNIVERSITY OF MARIBOR

## Odgovorni urednik / EDITOR-IN-CHIEF

Andrej PREDIN

## Uredniki / CO-EDITORS

Jurij AVSEC  
Miralem HADŽISELIMOVIĆ  
Gorazd HREN  
Peter VIRTič

## Izdajateljski svet in uredniški odbor / PUBLISHING COUNCIL AND EDITORIAL BOARD

**Zasl. prof. dr. Dali ĐONLAGIĆ,**

Univerza v Mariboru, Slovenija, **predsednik** / University of Maribor, Slovenia, **President**

**Prof. dr. Jurij AVSEC,**

Univerza v Mariboru, Slovenija / University of Maribor, Slovenia

**Zasl. prof. dr. Bruno CVIKL,**

Univerza v Mariboru, Slovenija / University of Maribor, Slovenia

**Prof. ddr. Denis ĐONLAGIĆ,**

Univerza v Mariboru, Slovenija / University of Maribor, Slovenia

**Prof. dr. Danilo FERETIĆ,**

Sveučilište u Zagrebu, Hrvatska / University in Zagreb, Croatia

**Doc. dr. Željko HEDERIĆ,**

Sveučilište Josipa Jurja Strossmayera u Osijeku, Hrvatska / Josip Juraj Strossmayer University  
Osijek, Croatia

**Izr. prof. dr. Miralem HADŽISELIMOVIĆ,**

Univerza v Mariboru, Slovenija / University of Maribor, Slovenia

**Doc. dr. Gorazd HREN,**

Univerza v Mariboru, Slovenija / University of Maribor, Slovenia

**Prof. dr. Roman KLASINC,**

Technische Universität Graz, Avstrija / Graz University Of Technology, Austria

**Prof. dr. Ivan Aleksander KODELI,**

Institut Jožef Stefan, Slovenija / Jožef Stefan Institute, Slovenia

**Prof. dr. Alfred LEIPERTZ,**

Universität Erlangen, Nemčija / University of Erlangen, Germany

**Prof. dr. Branimir MATIJAŠEVIČ,**

Sveučilište u Zagrebu, Hrvaška / University of Zagreb, Croatia

**Prof. dr. Borut MAVKO,**

Inštitut Jožef Stefan, Slovenija / Jozef Stefan Institute, Slovenia

**Prof. dr. Matej MENCINGER,**

Univerza v Mariboru, Slovenija / University of Maribor, Slovenia

**Prof. dr. Greg NATERER,**

University of Ontario, Kanada / University of Ontario, Canada

**Prof. dr. Enrico NOBILE,**

Università degli Studi di Trieste, Italia / University of Trieste, Italy

**Prof. dr. Andrej PREDIN,**

Univerza v Mariboru, Slovenija / University of Maribor, Slovenia

**Prof. dr. Aleksandar SALJNIKOV,**

Univerza Beograd, Srbija / University of Beograd, Serbia

**Prof. dr. Brane ŠIROK,**

Univerza v Ljubljani, Slovenija / University of Ljubljana, Slovenia

**Doc. dr. Andrej TRKOV,**

Institut Jožef Stefan, Slovenija / Jožef Stefan Institute, Slovenia

**Izr. prof. dr. Peter VIRTIČ,**

Univerza v Mariboru, Slovenija / University of Maribor, Slovenia

**Prof. dr. Koichi WATANABE,**

KEIO University, Japonska / KEIO University, Japan

**Prof. dr. Mykhailo ZAGIRNYAK,**

Kremenchuk Mykhailo Ostrohradskyyi National University, Ukrajina / Kremenchuk Mykhailo Ostrohradskyyi National University, Ukraine,

#### **Tehniška podpora / TECHNICAL SUPPORT**

Tamara BREČKO BOGOVČIČ,

Janko OMERZU

### **Izhajanje revije / PUBLISHING**

Revija izhaja štirikrat letno v nakladi 150 izvodov. Članki so dostopni na spletni strani revije - [www.fe.um.si/si/jet.html](http://www.fe.um.si/si/jet.html) / The journal is published four times a year. Articles are available at the journal's home page - [www.fe.um.si/en/jet.html](http://www.fe.um.si/en/jet.html).

Cena posameznega izvoda revije (brez DDV) / Price per issue (VAT not included in price):  
50,00 EUR

Informacije o naročninah / Subscription information: <http://www.fe.um.si/en/jet/subscriptions.html>

### **Lektoriranje / LANGUAGE EDITING**

Terry T. JACKSON

### **Oblikovanje in tisk / DESIGN AND PRINT**

Fotografika, Boštjan Colarič s.p.

### **Oblikovanje revije in znaka revije / JOURNAL AND LOGO DESIGN**

Andrej PREDIN

### **Ustanovni urednik / FOUNDING EDITOR**

Andrej PREDIN

Izdajanje revije JET finančno podpira Javna agencija za raziskovalno dejavnost Republike Slovenije iz sredstev državnega proračuna iz naslova razpisa za sofinanciranje domačih znanstvenih periodičnih publikacij / The Journal of Energy Technology is co-financed by the Slovenian Research Agency.

## ***Cena nafte na svetovnem trgu vse nižja in nižja***

Ponudba nafte na svetovnem trgu je trenutno zelo velika, saj jo ponujajo tako Rusija kot ZDA, Libija in ostali. To pomeni, da je trenutno ponudba mnogo večja od povpraševanja. Tako je cena za sodček (cca. 159 litrov) okoli 80 evrov. Predvideva se celo, da bo dosegla najnižjo točko, okrog 75 evrov za sodček. Praviloma bi bilo to za nas potrošnike vsekakor ugodno, saj bodo ponudniki primorani še nižati cene. Vendar pa, ker država regulira cene, to konkretno za nas ne pomeni nič kaj veliko znižanje cen, saj je naša država dvignila trošarine, tako da se je prodajna cena praktično ohranila na enakem nivoju kot do sedaj.

V Sloveniji se žal nič ne dogaja v smeri, da bi znižali energetske odvisnosti od tujega trga, predvsem pri tekočih in plinastih gorivih. Vse premalo je vzpodbud v tej smeri, ki bi seveda lahko tudi oživila slovensko gospodarstvo, da bi pričeli večati proizvodnjo in seveda domačo ponudbo alternativnih oblik tekočih goriv. Lahko bi, na primer, oživeli pridelavo in proizvodnjo bio-goriv iz lesne biomase, ki jo je ta trenutek zaradi žledoloma precej. Že povečana proizvodnja in domača poraba lesne biomase v obliki domačih sekancev in peletov bi lahko pomenila dodatni gospodarski zagon. Pa se žal nič ne zgodi, ker se v Sloveniji raje ukvarjamo z obrekovalnimi politikami (politikami) kot z resnimi temami. Tako žal recesiji v Sloveniji še ni videti konca.

Zdrava pamet v Sloveniji tako skoraj ne velja več, veljajo pa pravo, predpisi, procesne napake, kraje, korupcija in druge oslarije, ki našo ljubo državo vodijo v propad.

Andrej PREDIN



## ***The price of oil on the world market all lower and lower***

The supply of oil on the global market is currently very high, as it is offered by Russia and the US, Libya and others. At present, the supply is much greater than the demand. Consequently, the price per barrel (ca. 159 litres) is about €80; it is anticipated to reach its lowest point around €75 euros per barrel. As a rule, this would certainly be favorable for consumers, because providers will be forced to reduce their prices. However, because the Republic of Slovenia regulates fuel prices, this means anything but a significant price drop since the state has raised the excise duty so that the selling prices have practically remained unchanged.

In Slovenia, unfortunately, nothing is going in the direction of reducing energy dependence on foreign markets, specifically in liquid and gaseous fuels. There is a lack of incentives in this direction. However, it could aid in reviving the Slovenian economy, which had started to increase production and of course the domestic supply of alternative forms of liquid fuels. We could, for example, revive the production and the production of bio-fuels from biomass, especially considering the large amount of raw material left over from last winter's icestorm. An increased production and domestic consumption of wood biomass in the form of domestic wood chips and pellets could result in an additional economic boost. Unfortunately, nothing like this has happened, because Slovenia's politicians have spent so much time engaging in infighting and scandals instead of dealing with serious issues. Thus, unfortunately, the recession in Slovenia is no end in sight.

Savvy in Slovenia, so almost no longer applies, subject to the law, regulations, procedural error, theft, corruption and other crap that our dear to lead the country to ruin.

Andrej PREDIN

# **Table of Contents / Kazalo**

## **Formula for calculation of magnetic field strength over the middle of the gap of a bipolar suspended iron separator /**

Enačba za izračun jakosti magnetnega polja po sredini reže bipolarnih suspendiranih separatorjev železa

*Mykhaylo Zagirnyak* . . . . . 11

## **Turbine sealing steam heat recovery with dynamic Stirling engines /**

Izraba toplote tesnilne pare turbine z dinamičnimi Stirling motorji

*Dušan Strušnik, Milan Marčič, Jurij Avsec* . . . . . 17

## **Low enthalpy systems in geothermal energy /**

Nizko entalpijski sistemi v geotermalni energiji

*Renato Strojko* . . . . . 35

## **Review of energy regulations on solar energy (PV) in Slovenia and Austria /**

Pregled energetske regulative za sončno energijo (PV) v Sloveniji in Avstriji

*Franjo Pranjič* . . . . . 47

## **Numerical analysis of lift and pressure coefficients of an airfoil: Ansys vs SolidWorks /**

Numerična analiza koeficienta vzgona in tlaka profila krila: Ansys in SolidWorks

*Igor Spaseski, Marko Pezdevšek, Igor Ščuri, Matej Fike, Gorazd Hren* . . . . . 63

**Instructions for authors** . . . . . 75

# FORMULA FOR CALCULATION OF MAGNETIC FIELD STRENGTH OVER THE MIDDLE OF THE GAP OF A BIPOLAR SUSPENDED IRON SEPARATOR

## ENAČBA ZA IZRAČUN JAKOSTI MAGNETNEGA POLJA PO SREDINI REŽE BIPOLARNIH SUSPENDIRANIH SEPARATORJEV ŽELEZA

Mykhaylo Zagirnyak<sup>✉</sup>

**Keywords:** suspended electromagnetic separator, magnetic field strength, conformal transformation

### **Abstract**

A formula providing the possibility of calculating with sufficient accuracy the strength of the magnetic field over the middle of the inter-polar gap formed by sloping surfaces of pole pieces of U-type electromagnets of suspended iron separators is presented.

### **Povzetek**

Predstavljena je enačba, ki zagotavlja možnost dovolj točnega izračuna jakosti magnetnega polja po sredini reže med poloma, ki ga tvorijo nagnjene površine delov polov elektromagnetov U-tipa suspendiranih separatorjev železa.

---

✉ Corresponding author: Mykhaylo Zagirnyak, D.Sc. (Eng.), Prof., Tel.: +38 05366 36218, Fax: +38 05366 36000, Mailing address: Kremenchuk Mykhailo Ostrohradskiy National University Vul. Pershotravneva, 20, 39600, Kremenchuk, Ukraine, E-mail address: [mzagirn@kdu.edu.ua](mailto:mzagirn@kdu.edu.ua)

## 1 INTRODUCTION

At present, the extraction of foreign ferromagnetic objects from various bulk materials transported by belt conveyers is carried out by dedicated direct current electromagnets (suspended iron separators), [1, 2]. Suspended iron separators based on U-type bipolar magnetic systems are a common type of such electromagnets (Figure 1).

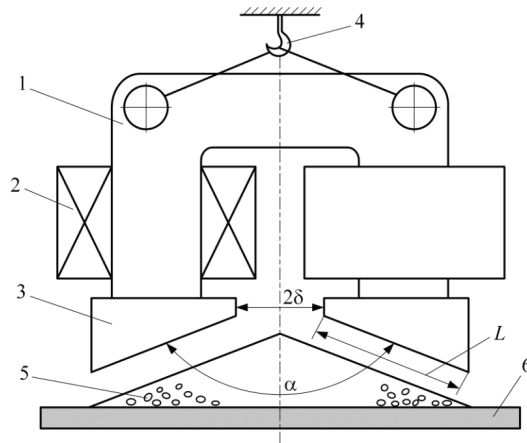


**Figure 1:** Suspended electromagnetic separator

One of the critical stages of designing suspended iron separators is the calculation of the magnetic field in the inter-polar zone, where the separated bulk material is located. In this case, field strength and its gradient, [2–6], are the basic calculation values. A number of methods of different degrees of accuracy are offered in Smolkin and Sayko's paper, [7], to determine these values at all the points of inter-polar space of suspended electromagnetic separators. However, these methods result in rather complicated calculation formulas, which make their use in practical design difficult. Calculation difficulties (e.g. necessity of solution of equations of an implicit form) occur due to taking into account the angle  $\alpha \neq 180^\circ$  (Figure 1) between the operating surfaces of pole pieces forming the basic magnetic flux through the working zone of the suspended iron separator. The following designations are assumed in Figure 1: 1 – magnetic circuit; 2 – magnetizing winding; 3 – pole pieces; 4 – suspension; 5 – bulk material; 6 – conveyor belt.

It should be mentioned that at the preliminary stages of designing suspended iron separators, as a rule, the knowledge of magnetic field strength and its gradient is required only for the points of the vertical of the middle of the inter-polar gap. Obviously, it is the most difficult place for extraction due to the maximum thickness of the layer of the separated material, [1–3], i.e. there is often no necessity to calculate the strength distribution across the whole inter-polar space during preliminary calculation. This is why the problem of this paper consists of obtaining the formula of magnetic field strength for the points situated over the middle of the gap between sloping pole pieces of U-type magnetic system. This formula should be simple for practical calculation and to provide accuracy sufficient for preliminary design calculations.

## 2 INVESTIGATION MATERIAL

With the aim of solving the posed problem, it should be taken into consideration that, as shown in [8], the calculation of magnetic field of pole pieces lying in the same plane ( $\alpha = 180^\circ$ ) can be reduced to the calculation of a plane-parallel field of two infinite plates (Figure 2); the magnetic potential difference between them equals  $U_0$ ; the magnetic potentials difference between pole pieces and their geometry (width  $L$  and gap  $\delta$ ) equals to the corresponding dimensions of the magnetic system. In the case of the same-plane poles, the field strength in the middle of inter-polar gap ( $x = 0, y \geq 2$ , Figure 2) has one component (horizontal) that can be recorded on the basis of corresponding formulas from [8, 9], with the assumed dimensions designation (Figure 2), in the form:

$$H_0(y) = U_0 \frac{0,5}{K(k)} \cdot \frac{(L + \delta)}{\sqrt{\delta^2 + y^2} \sqrt{(L + \delta)^2 + y^2}} \quad (2.1)$$

where  $y$  is the vertical distance from the poles plane to the point at which the strength is determined;  $K(k)$  is the first-type complete elliptic integral with module  $k = \delta / (L + \delta)$ .

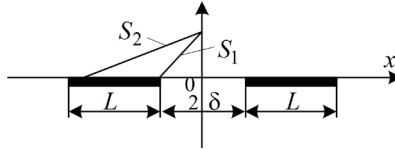


Figure 2: Two infinite plates

If values  $S_1$  and  $S_2$ , i.e. distances to the analyzed point from the internal and the external edges, respectively, of pole-plates are introduced (Figure 2):

$$S_1 = \sqrt{\delta^2 + y^2}, \quad S_2 = \sqrt{(L + \delta)^2 + y^2},$$

then formula (2.1) can be converted to the form:

$$H_0(y) = U_0 \frac{0,5}{K(k)} \cdot \frac{(L + \delta)}{(S_1 \cdot S_2)} \quad (2.2)$$

The magnetic field in the inter-polar zone can also be considered plane-parallel for poles having an angle between the pieces surfaces of less than  $180^\circ$ , [7]. Let us assume that in this case the magnetic field strength at the points over the middle of the inter-polar gap (axis  $y$  in Figure 3) is also determined by formula (2.2) in which, analogously to the previous one,  $S_1$  and  $S_2$  are presumed to be distances from corresponding pole edges to the analyzed point (Figure 3):

$$S_1 = \sqrt{\delta^2 + (y - \delta \operatorname{ctg}(\alpha/2))^2},$$

$$S_2 = \sqrt{(\delta + L \sin(\alpha/2))^2 + (y - \delta \operatorname{ctg}(\alpha/2) - L \cos(\alpha/2))^2}, \quad (2.3)$$

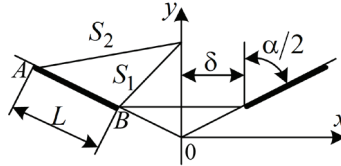


**Figure 3:** Two plane-parallel plates having the angle  $\alpha$  between their surfaces

As to multiplier  $(L + \delta)$  and module  $k$ , contained in (2.2), corresponding values for sloping pole pieces can be determined by distances obtained when the upper plane of pole pieces crosses the vertical of the middle of inter-polar gap (line  $ABO$  in Figure 3), i.e. in this case, dimension  $BO = \delta/\sin(\alpha/2)$  represents value  $\delta$ , and dimension  $AO = [L + \delta/\sin(\alpha/2)]$  is taken instead of  $(L + \delta)$ , which yields

$$k = \frac{\delta/\sin(\alpha/2)}{L + \delta/\sin(\alpha/2)} = \frac{\delta}{\delta + L \sin(\alpha/2)} \quad (2.4)$$

Thus, taking the above said into consideration, the following can be recorded for magnetic field strength at the points over the middle of the inter-polar gap of sloping poles

$$H_\alpha(y) = U_0 \frac{0,5}{K(k)} (L + \delta/\sin \alpha/2) / (S_1 S_2) \quad (2.5)$$

where  $S_1, S_2$  and  $k$  are taken from (2.3) and (2.4), respectively.

When parameters  $L, \delta, \alpha$  are known, calculation according to (2.5) does not present any difficulties if the following relation from [10] is used for an approximate calculation of  $K(k)$  (true with accuracy up to the fourth decimal):

$$K(k) = \sum_{i=0}^2 (1 - k^2)^i \left[ a_i + b_i \operatorname{h} \left( \frac{1}{1 - k^2} \right) \right] \quad (2.6)$$

where  $a_0 = 1.3862944$ ;  $a_1 = 0.1119723$ ;  $a_2 = 0.0725296$ ;  $b_0 = 0.5$ ;  $b_1 = 0.1213478$ ;  $b_2 = 0.0288729$ .

To substantiate formula (2.5), it should be noted that qualitative dependences  $H_\alpha(y)$  on certain parameters (the case of sloping plates of poles) are to be identical to analogous dependences for the case of single-plane poles. This identity is provided by the assumed similarity of formula structures for  $H_0(y)$  and  $H_\alpha(y)$ . It should also be mentioned that in the case of  $\alpha = 180^\circ$ , formula (5) transforms into an accurate formula (2.2).

### 3 EXPERIMENTAL VERIFICATION

Experimental verification of formula (2.5) was carried out with a physical model of a suspended iron separator P160 (scale 1:5). Corresponding data are given in Table 1; they show good coincidence of the results of calculation according to the proposed formula with the results of the experiment. Furthermore, formula (2.5) was verified by means of comparison of the experimental data for a suspended iron separator P100M given in [7] with the results of the calculation according to (2.5) for corresponding dimensions (Table 2). As [7] does not contain a numerical value  $U_0$  for suspended iron separator P100M, the calculated reduced strength  $H = H_\alpha(y)/U_0$  is included in Table 2. As to the degree of certainty of the calculation, it was determined according to the ratio of the experimental value of magnetic field strength from [7] to  $H$ , which, according to (2.5), is to be a constant value not depending on  $y$ . Analysis of the corresponding results shows that formula (2.5) provides acceptable accuracy for practical calculations.

**Table 1:** Magnetic field strength over the middle of inter-pole gap of a physical model of suspended iron separator P160 ( $\delta = 24$  mm,  $L = 106.5$  mm,  $\alpha = 155^\circ$ ,  $U_0 = 7695.34$  A)

Distance $y$ , mm	Field strength, A/m		Error, %
	calculated according to formula (5)	Experimental	
15	159174	153585	+3.64
20	129938	128120	+1.42
25	107234	105838	+1.32
30	90209	89127	+1.21
35	77293	77190	+0.13
40	67261	67641	-0.56
45	59278	60479	-1.99
50	52780	54113	-2.46
55	47390	48542	-2.37

**Table 2:** Error of the calculation of magnetic field strength in the operating zone of suspended iron separator P100M ( $\delta = 85.4$  mm,  $L = 350$  mm,  $\alpha = 120^\circ$ ) over the middle of the inter-polar gap

$y$ , mm	Strength values		Ratio $H_y / H^*$ , A	Mean value of ratio $H_y / H^*$ , A	Deviation from the mean value, %
	given according to calculation $H^*$ , 1/M	absolute, from experience $H_y$ , A/m			
42.7	4.46394	1880	4229.44	3852.16	+9.8
92.7	3.8699	1530	3953.59		+2.6
142.7	2.8701	10970	3822.16		-0.8
192.7	2.17154	7940	3656.38		-5.1
242.7	1.70315	6130	3599.22		-6.6

## 4 CONCLUSIONS

The proposed formula can be recommended for preliminary stages of the calculation of suspended iron separators, when it is necessary to determine the magnetic field strength at the points over the middle of the inter-polar gap of a U-type magnetic system.

## References

- [1] **J. Svoboda**: *Magnetic methods for the treatment of minerals*, Elsevier, 1987, 692 p.
- [2] **M. V. Zagirnyak, Yu. A. Branspiz, I. A. Shvedchikova**: *Magnetic separators. Design problems. Monograph*, Kyiv, Technika, 2011, 224 p. (in Russian)
- [3] **M. V. Zagirnyak, Yu. A. Branspiz, R. M. Pai, S. A. Nasar**: *Forces in pilley-type electromagnetic separators*, IEEE Transactions on magnetics, Vol.Mag-22 No. 1, January 1986, pp. 63–67.
- [4] **R. D. Smolkin**: *Calculation of magnetic field strength and electromagnetic ponderomotive force of separators*, IEEE Transactions on magnetics, Vol.38 No. 3, May 2002, pp. 1528–1533.
- [5] **R. D. Smolkin**: *Calculation and analysis of the magnetic force acting on a particle in the magnetic field of separator. Analysis of the equations used in the magnetic methods of separation*, IEEE Transactions on magnetics, Vol.42 No. 11, November 2006, pp. 3682–3693.
- [6] **R. D. Smolkin**: *Analysis of magnetic fields and circuits in separators with plane-parallel and plane-meridian symmetry*, IEEE Transactions on magnetics, Vol.44 No. 8, August 2008, pp. 1990–2001.
- [7] **R. D. Smolkin, O. P. Sayko**: *Magnetic field calculation of two-pole magnetic systems of suspending electromagnetic separators*, Izv.vuzov. Electromechanica, 1989, No. 3, pp. 12–20. (in Russian)
- [8] **M. S. Zakharova, R. D. Smolkin**: *About the calculation of the two-pole electromagnetic separators*, Enrichment Mineral Resources, No. 11, pp. 51–56, 1972. (in Russian)
- [9] **K. J. Binns, P. J. Lawrenson, C. W. Trowbridge**: *The analytical and numerical solution of electric and magnetic fields*; John Wiley & Sons Publishers, 1992, 486 p.
- [10] **M. Abramowitz, I. Stegun**: *Handbook on special functions*, Moscow, Nauka, 1979. 830 p. (in Russian)



# TURBINE SEALING STEAM HEAT RECOVERY WITH DYNAMIC STIRLING ENGINES

## IZRABA TOPLOTE TESNILNE PARE TURBINE Z DINAMIČNIMI STIRLING MOTORJI

Dušan Strušnik<sup>✉</sup>, Milan Marčič, Jurij Avsec

**Keywords:** analysis, Stirling engine, heat, working gas, sealing steam, steam turbine, regenerator, efficiency, isochoric compression

### **Abstract**

This paper presents the possibilities of sealing steam heat recovery in a steam condensation turbine with the use of dynamic Stirling engines. The installation of dynamic Stirling engines into the turbine sealing steam system allows the recovery of sealing steam heat and the generation of electrical energy. The Stirling engine dynamics are expressed with a built-in working gas storage tank and working gas flow control to ensure adequate power output of the Stirling engine. The working gas quantity in the engine is controlled with regard to the available turbine sealing steam heat. Via the measurement of the turbine sealing steam quantity and quality, a model of the working gas pressure conditions in the Stirling engine is designed. The engine responsiveness at various working gas quantities and types is analysed.

### **Povzetek**

V članku bomo predstavili možnosti izrabe toplote tesnilne pare parne kondenzacijske turbine z dinamičnim Stirling motorji. Z vgraditvijo dinamičnih Stirling motorjev v armaturo tesnilne pare tur-

---

<sup>✉</sup> Corresponding author: Dušan Strušnik, Energetika Ljubljana d.o.o. enota TE-TOL, Toplarniška ulica 19, 1000 Ljubljana, Slovenija.

E-mail address: [dusan.strusnik@gmail.com](mailto:dusan.strusnik@gmail.com).

bine bomo izkoriščali toploto tesnilne pare in pridobivali električno energijo. Dinamika Stirling motorja se izraža z vgrajenim hranilnikom in regulacijo količine delovnega plina, ki poskrbi za ustrezno moč Stirling motorjev. Količina delovnega plina v motorju se uravnava glede na razpoložljivi toploto tesnilne pare turbine. S pomočjo opravljenih meritev količine in kvalitete tesnilne pare turbine, bomo izdelali model tlačnih razmer delovnega plina v Stirling motorju. Analizirali bomo odzivnost motorja pri različnih količinah in vrstah delovnih plinov.

## 1 INTRODUCTION

Sealing steam is steam-generated process during a steam turbine operation. Due to the leakage of high-pressure labyrinth seals, a constant sealing steam flow is created, used for the sealing of the low-pressure labyrinth seals, whereby the remaining flow is directed to the sealing steam condenser. The steam condenses in the sealing steam condenser and emits heat to the network water used for district heating. With the installation of Stirling engines into the sealing steam system, it is possible to produce thermal energy, as well as electrical energy. Stirling engines have been widely applied in various energy-related solutions, [1–5].

A Stirling engine is a heat engine using hot air and is considered to be one of the simplest engines and is the only one to use external combustion, in contrast to other engines. Its design is simple; it requires no fuel injection system and can use various types of fuels (biomass, coal, methane, hydrogen, etc.). The advantages of a Stirling engine in comparison with other heat engines are higher efficiency, lower environmental impact, no explosions taking place in a cylinder, and lower levels of noise and vibrations, [6]. One particular feature of Stirling engines is their heat regenerator, located in the engine cylinder air passage. The regenerator increases the engine efficiency by accumulating a portion of the heat of the working gas passing between the Stirling engine cylinders.

There are several types of engines, [7–10]. In practice, the alpha, beta, gamma and the combined configurations are most frequently used. The operating principle of all configurations is based on thermodynamic laws of working gas expansion and compression. In our case, a gamma configuration of the Stirling engine was chosen because the engine design allows the cylinders to be installed in separate locations.

The Stirling engine gamma configuration has two separate cylinders (a hot and a cold cylinder), [9]. The hot cylinder is mounted into the sealing steam system, whereas the cold cylinder is mounted outside the system and is additionally cooled. In our case, demineralised water (18°C) will be used for cooling to compensate for the losses during the process. A heat flow is created between the hot and the cold cylinders. The Stirling engine's power may be changed through a temperature difference of the hot and cold ends of the engine, through a compression ratio and the type and mass of the working gas. Furthermore, the selection of working gas impacts the engine's power, because working gases have different specific heat ratios.

Due to the structural properties of materials, the Stirling engine is designed for a particular gas, thus making any subsequent change in the engine working gas impossible. However, a change in the amount of the working gas during engine operation is possible. Such a change and a temperature change lead to a change in the pressure ratio in the engine, [11]. Everything indicated above must be taken into consideration in the engine design and construction.

## 2 MOUNTING AND CONTROL OF STIRLING ENGINES IN THE TURBINE SEALING STEAM SYSTEM

Due to the large amount of available heat of the turbine sealing steam, two Stirling engines operating in parallel and sharing a common generator will be installed into the sealing steam system. Each engine is built into its own system, allowing easier engine handling and operation. Two regulation circles will ensure the rational production of the Stirling engine's output. The first regulation circle will control the sealing steam quantity in the system in accordance with the energy needs. The second regulation circle will control the amount of the working gas in the Stirling engine in accordance with the available quantity of sealing steam. The mounting of the Stirling engine in the sealing steam system is illustrated in Figure 1.

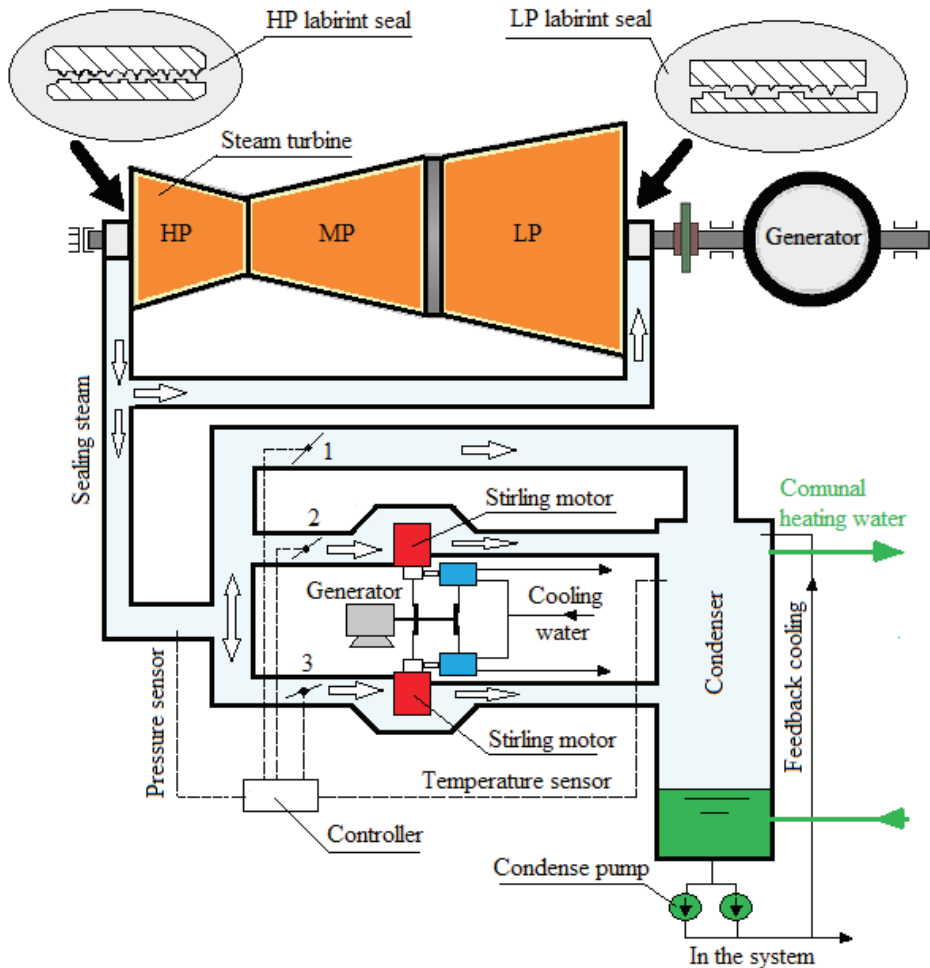
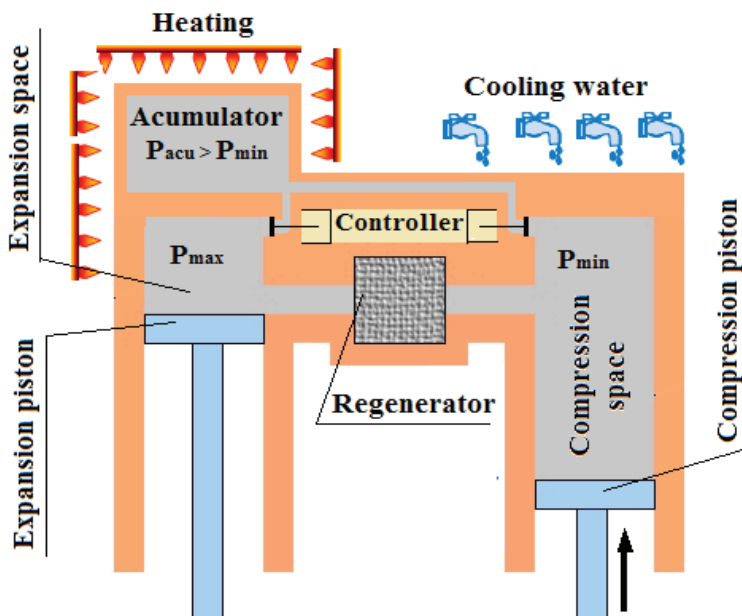


Figure 1: Mounting of Stirling engines into the turbine sealing steam system

The first regulation circle will control the position of Throttle 1, 2 and 3 in accordance with the energy needs (Figure 1). In normal operation, the position control of Throttles 2 and 3 maintains the required sealing steam pressure, varying with the change in the turbine load. Throttle 1 is in the closed position, and Throttles 2 and 3 control the amount of the sealing steam for the Stirling engine operation. If the demand for district heating increases, the controller will start opening Throttle 1 and closing Throttles 2 and 3 in accordance with the required sealing steam pressure and the network water temperature in the condenser. This will lead to an increase in the amount of the sealing steam towards the condenser and a decrease in the amount of sealing steam towards the Stirling engines.

In accordance with the amount of the sealing steam, the second regulation circle will change the working gas quantity and, therefore, the Stirling engine's power. A change in the amount of the Stirling engine's working gas will be carried out by placing an accumulation reservoir between the expansion and the compression space to control the amount of the working gas in the engine in accordance with the available sealing steam quantity. If less sealing steam is available, the working gas will be sent to the accumulation reservoir from the cylinder expansion area at a higher pressure. Moreover, conversely, with an increased amount of the sealing steam, the engine's power will be increased by feeding the working gas from the accumulation reservoir into the compression area of the engine. The control of engine working gas will be performed by means of two control valves, as illustrated in Figure 2. The accumulation reservoir has to be located on the hot cylinder in order to ensure that the accumulation reservoir pressure is always higher than the pressure in the compression cylinder.



**Figure 2:** Gamma-type Stirling engine with the working gas control

The working gas serves as a substance to which heat is added or removed, resulting in the working gas expansion or compression with the internal mechanism being in motion. The choice of the working gas has a direct impact on the Stirling engine's efficiency, power, safety and general operation. Working gases have been widely applied in various energy related issues, [11-14]. The influencing factors in the working gas selection include price, flammability, viscosity, thermal conductivity, diffusivity, specific heat and electrical efficiency. Electrical efficiency is the ratio between the generated electrical energy and the Stirling engine input energy. It is expected that electrical efficiency varies according to the gas constant, i.e. the highest at air and the lowest at hydrogen, [11]. The thermodynamic properties of the working gases used in Stirling engines are indicated in Table 1.

**Table 1:** Working gas properties

Name	Symbol	Density	Gas constant
Helium	$He$	0.1785 kg/m <sup>3</sup>	2078 J/kgK
Air		1.2 kg/m <sup>3</sup>	259.8 J/kgK
Acetylene	$C_2H_2$	1.097 kg/m <sup>3</sup>	319.6 J/kgK
Ammonia	$NH_3$	0,73 kg/m <sup>3</sup>	488.3 J/kgK
Hydrogen	$H_2$	0,08987 kg/m <sup>3</sup>	4122 J/kgK
Freon	$CF_2Cl_2$	5.11 kg/m <sup>3</sup>	68.8 J/kgK

### 3 MATHEMATICAL ANALYSIS AND CALCULATION OF STIRLING ENGINE'S POWER OUTPUT

The Stirling engine can be used as a machine, a heat pump or a cooler, installed between a heat source (a heated body) and a heat sink (a cold body). The temperature difference between the bodies leads to a heat flow used by the heat engine. The regeneration that increases the efficiency of the engine will be taken into consideration in the calculation. Mathematical analysis has been widely applied in various energy related issues, [15–17].

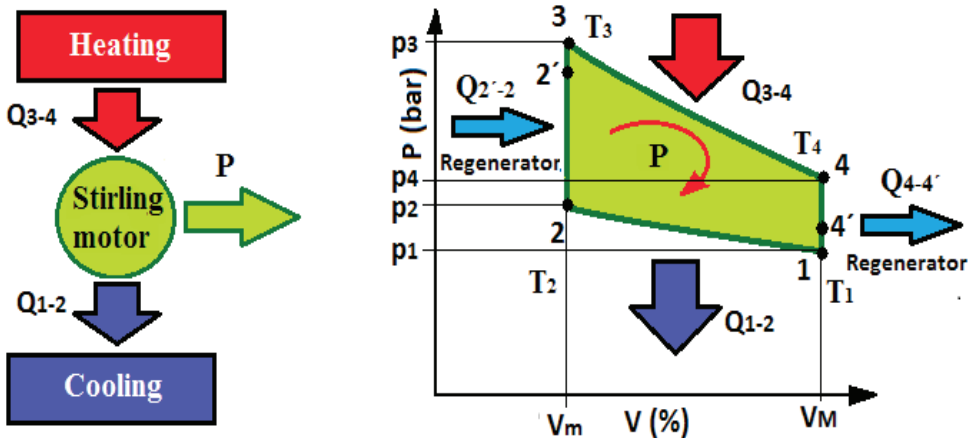


**Figure 3:** Conversion of the working gas and generation of the Stirling engine work

### 3.1 Stirling engine mathematical analysis

States 1 to 2 Isothermal compression (Figure 3).

The working fluid is in contact with the cold surface, where the working gas volume of the Stirling engine is reduced. The Boyle-Mariott law applies to the isothermal compression:

$$p \cdot V = m \cdot R \cdot T = \text{const} \quad (3.1)$$

where  $p$  – working gas pressure (Pa),

$V$  – working gas volume (m<sup>3</sup>),

$m$  – working gas mass (kg),

$R$  – specific gas constant (J/kgK),

$T$  – gas temperature (K).

The Stirling engine output heat ( $Q_{1-2}$ ) is calculated using the following equation:

$$Q_{1-2} = p_1 \cdot V_1 \cdot \ln \frac{1}{\pi} = m \cdot R \cdot T_1 \cdot \ln \frac{1}{\pi} \quad (3.2)$$

where:  $Q_{1-2}$  – engine output heat (J),

$p_1$  – working gas pressure at point 1 (Pa),

$T_1$  – working gas temperature at point 1 (Pa),

$V_1$  – working gas volume at point 1 (m<sup>3</sup>),

$\pi$  – compression ratio of working gas conversion.

States 2 to 3 Isochoric compression (Figure 3).

The working gas is heated by means of the accumulated regenerator of the Stirling engine, where the temperature is isochorically increased from State  $T_1$  to State  $T_4$  (Figure 3). At this point, the working gas pressure is the highest. The accumulated regenerator input heat ( $Q_{1-2}$ ) is calculated using the following equation:

$$Q_{2-3} = V_2 \cdot \left( \frac{p_3 - p_2}{\kappa - 1} \right) = m \cdot c_v \cdot (T_3 - T_2) \quad (3.3)$$

where:  $V_2$  – working gas volume at point 2 (m<sup>3</sup>),

$p_2$  – working gas pressure at point 2 (Pa),

$p_3$  – working gas pressure at point 3 (Pa),

$\kappa$  – ratio of specific heats,

$c_v$  – working gas specific heat at a constant volume (J/(kgK)),

$T_2$  – working gas temperature at point 2 (K),

$T_3$  – working gas temperature at point 3 (K),

Regeneration entails a decrease in the input heat on account of the working gas regenerated heat.

The regeneration rate ( $\sigma$ ) indicates how much heat has been regenerated in a particular circular process, and it is calculated using the following equation:

$$\sigma = \frac{T_{2'} - T_2}{T_3 - T_2} = \frac{T_3 - T_{4'}}{T_3 - T_2} \quad (3.4)$$

where:  $T_{2'}$  - working gas temperature at point 2' (K),

$T_{4'}$  - working gas temperature at point 4' (K).

The thermal efficiency of the circular process, without a heat regenerator ( $\eta_t$ ) is calculated:

$$\eta_t = \frac{(Q_{3-4} - Q_{1-2})}{(Q_{3-4} + Q_{2-3})} \quad (3.5)$$

where:  $Q_{3-4}$  – input heat of the process 3-4 (J),

The thermal efficiency of the circular process with a heat regenerator ( $\eta_{t,reg}$ ) is calculated:

$$\eta_{t,reg} = \frac{(Q_{3-4} - Q_{1-2})}{Q_{3-4}} = 1 - \frac{T_2}{T_3} \quad (3.6)$$

States 3 to 4 (Figure 3) Isothermal expansion.

The working gas is in contact with the heated surface, where the volume of the Stirling engine working gas is increased. The expansion piston performs the work, the volume increases, and the pressure drops at the working gas maximum temperature ( $T_4$ ). The Boyle-Mariott law applies to isothermal expansion (Equation 3.1).

The input heat of the process ( $Q_{3-4}$ ) is calculated:

$$Q_{3-4} = p_3 \cdot V_3 \cdot \ln \pi = m \cdot R \cdot T_4 \cdot \ln \pi \quad (3.7)$$

where:  $V_3$  – working gas volume at point 4 (m<sup>3</sup>).

The pressure at working point 4 ( $p_4$ ) is calculated:

$$p_4 = \frac{p_3 \cdot V_3}{V_4} = \frac{p_3}{\pi} \quad (3.8)$$

where:  $V_4$  – working gas volume at point 4 (m<sup>3</sup>)

State 4-1 (Figure 3) Isochoric expansion.

The working gas emits the heat to the regenerator that accumulates it, and it is cooled down from state  $T_4$  to state  $T_{4'}$  (Figure 3). The regenerator output heat ( $Q_{4-4'}$ ) equals the regenerator input heat ( $Q_{2-2'}$ ), multiplied by the regeneration loss ( $\eta_e$ ), and is calculated:

$$Q_{4-4'} = V_4 \cdot \frac{(p_{4'} - p_4)}{(\kappa - 1)} = m \cdot c_v \cdot (T_{4'} - T_4) = Q_{2'-2} \cdot \eta_e \quad (3.9)$$

where:  $p_{4'}$  - working gas pressure at point 4' (Pa),

$p_4$  – working gas pressure at point 4 (Pa).

Calculation of power

The Stirling engine’s power ( $P$ ) is the difference between the engine input and output heat multiplied by a loss factor ( $\eta_{em}$ ). The Stirling engine’s power output is calculated:

$$P = (Q_{3-4} - Q_{1-2}) \cdot \eta_{em} \tag{3.10}$$

The Stirling engine’s efficiency ( $\eta$ ) is the ratio between the work done and the input heat flow and is calculated using the following equation:

$$\eta = \frac{m \cdot R \cdot \ln \pi \cdot (T_4 - T_1) \cdot V}{m \cdot V \cdot c_v \cdot (T_4 - T_1) + R \cdot T_4 \cdot \ln \pi} = \frac{\ln \pi (T_4 - T_1) \cdot (\kappa - 1)}{(T_4 - T_1) + T_4 \cdot \ln \pi \cdot (\kappa - 1)} \tag{3.11}$$

**3.2 Stirling engine power calculation**

In order to calculate the Stirling engine’s power, the quality and quantity of the sealing steam of a condensation turbine at a Slovenian district heating plant were analysed. The sealing steam pressure oscillation was established ranging between 1.7 bar to 2.4 bar or 2.1 bar on average in a two-month period. The pressures are absolute. The sealing steam temperature varies between 260 °C and 300 °C and amounts to 280 °C on average in a two-month period. The sealing steam quantity varies between 1.2 kg/s and 2 kg/s. After the establishment of the quality of the sealing steam, heat can be determined by means of the enthalpy differential to be used for the operation of the Stirling engines. The enthalpy differential (Points 1 and 2) is illustrated in Figure 4.

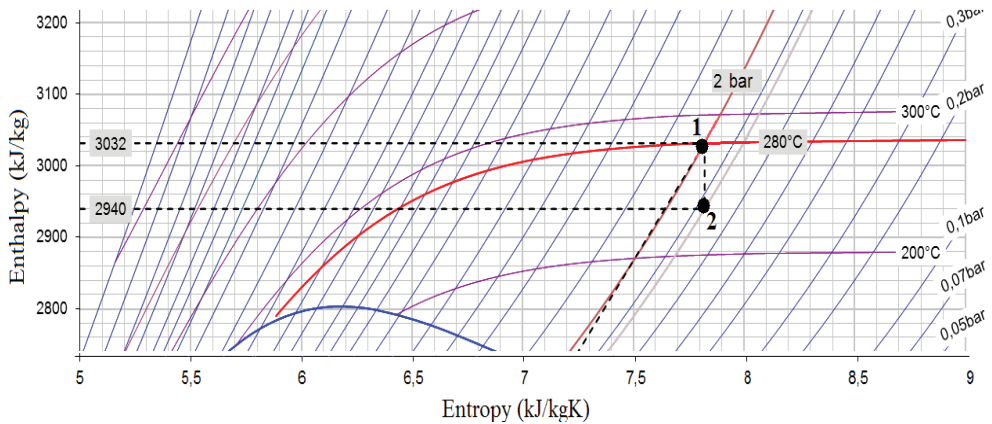


**Figure 4:** Sealing steam enthalpy differential used for the operation of the Stirling engines

If a drop in enthalpy of 92 kJ/kg is multiplied by the quantity of the sealing steam (1.6 kg/s), the power output to be used by the Stirling engine is obtained, and it amounts to 147 kW. If the sealing steam heat is used when a portion of the steam is directly led to a condenser via System 1 (Figure 1) 0.8 kg/s of the sealing steam or 74 kW of power may be used. A Stirling engine capable of using the sealing steam heat from 70 kW to 140 kW has to be designed. Considering that two Stirling engines operating in parallel will be mounted into the sealing steam system, the engine dimensions have to be such as to ensure the use of the sealing steam heat from 35 kW to 70 kW. Helium has been chosen as the Stirling engine working gas. The thermodynamic states of the working gas (helium)



at points indicated in Figure 3 were calculated using the equations indicated in Chapter 3.1. The results are illustrated in Table 2.

**Table 2:** Thermodynamic states of helium by point when using 35 kW and 70 kW

Name	Symbol	At 35 kW	At 70 kW
Minimum temperature	$T_1$	291 K	291 K
Maximum temperature	$T_4$	535 K	567 K
Expanded gas pressure	$p_1$	3.7093x10 <sup>5</sup> Pa	7x10 <sup>5</sup> Pa
Gas pressure, Pa	$p_2$	14.837x10 <sup>5</sup> Pa	28x10 <sup>5</sup> Pa
Compressed gas pressure	$p_3$	27.278x10 <sup>5</sup> Pa	54.557x10 <sup>5</sup> Pa
Gas pressure	$p_4$	6.8196x10 <sup>5</sup> Pa	13.639x10 <sup>5</sup> Pa
Expanded gas volume	$V_1$	0.037022 m <sup>3</sup>	0.037022 m <sup>3</sup>
Compressed gas volume	$V_2$	0.009255 m <sup>3</sup>	0.009255 m <sup>3</sup>
Compression rate	$\pi$	4	4
Helium specific heat ratio	$\kappa$	1.66	1,66
Mass of the gas in the system	$m$	0.02271 kg	0.042856 kg

Once the thermodynamic states of the working gas (helium) are known, the heat levels of the process, the engine's power output and the Stirling engine's thermal efficiency can be calculated. The results are indicated in Table 3.

**Table 3:** Heat, power output and efficiency at 35 kW and 70 kW

Name	Symbol	At 35 kW	At 70 kW
Process input heat	$Q_{3-4}$	35 kW	70 kW
Process output heat	$Q_{1-2}$	19.037 kW	35.926 kW
Regeneration heat	$Q_{2-3}$	17.446 kW	37.241 kW
Engine power output	$P$	15.483 kW	33.051 kW
Thermal efficiency with regeneration	$\eta_{t,reg}$	0.44	0.47

The results show that if using 70 kW of the sealing steam heat, the Stirling engine generates 33.051 kW of power and reaches 47% efficiency. If the Stirling engine uses 35 kW of the sealing steam heat, it generates 15.483 kW of power and reaches 44% efficiency. As two Stirling engines are mounted in the sealing steam system, the total maximum power is 66.102 kW and the minimum power 30.966 kW.

## 4 STIRLING ENGINE MODELLING

The Stirling engine responsiveness to a change in the sealing steam quantity will be established through modelling. The model is designed using the Matlab-Simulink software tool and comprises the main programme and subprograms (the main program interconnects the subprograms). The subprograms compute the sought values at a specific order. Figure 5 illustrates the Stirling model.

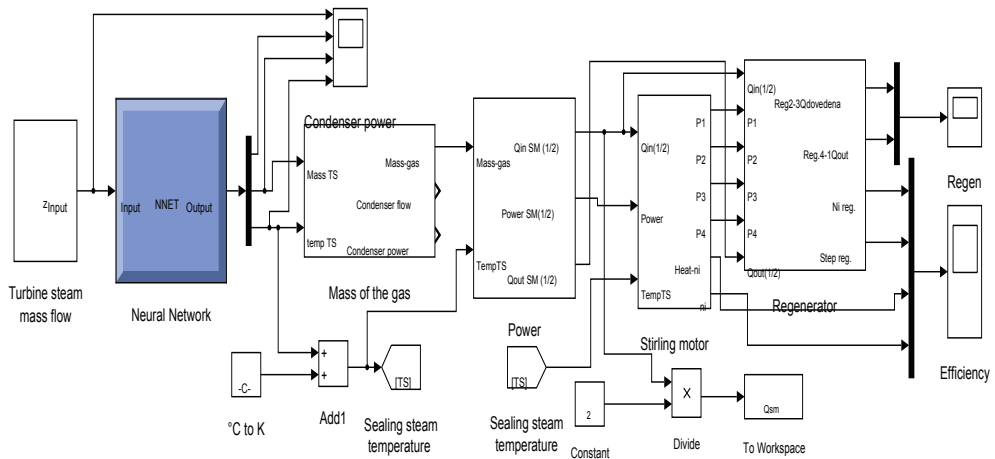


Figure 5: Stirling engine model, [18]

The neural network subprogram is a pre-trained network. The input data was given in a matrix format [1×2366]. The output data in a matrix format [3×2366] describe the sealing steam temperature, quantity and pressure. A neural network was designed on the basis of the input data of one group (amount of steam admitted to the turbine) and the results in three groups (sealing steam temperature, quantity and pressure). The neural network contains two groups of 90×10 hidden neurons. Other authors has been widely applied the neural network in various energy related issues, [19-22]. The neural network architecture is shown in Figure 6.

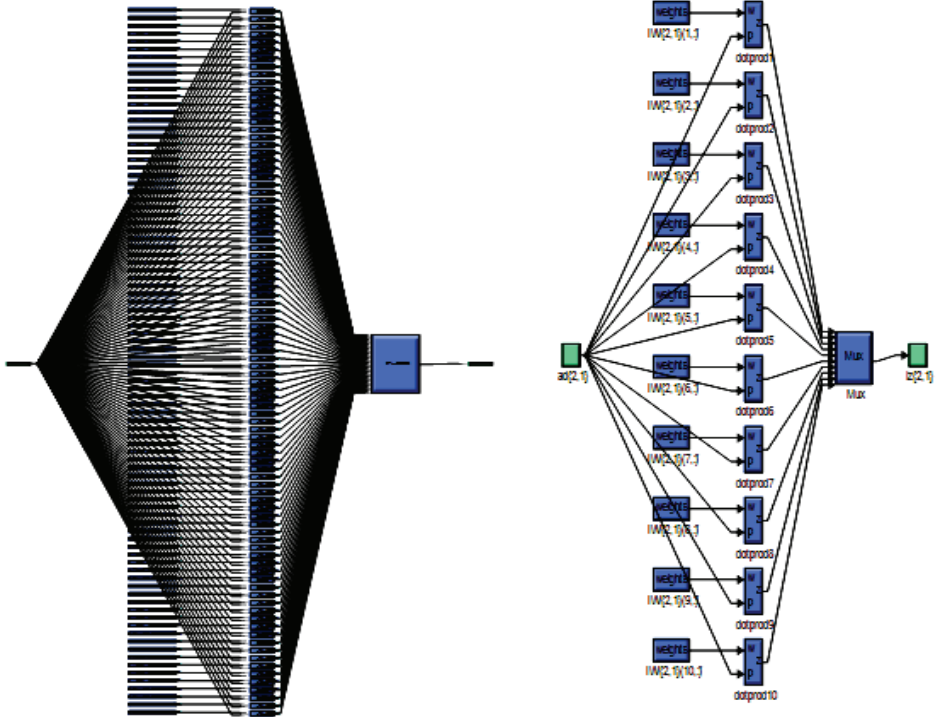
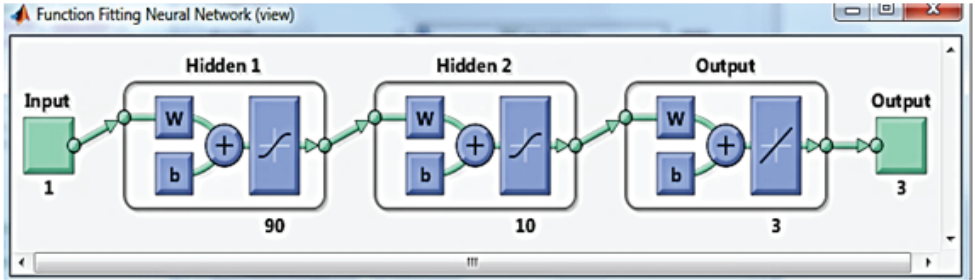


Figure 6: Neural network architecture, [18]

Figure 7 shows the results of the input–output data fit of the trained neural network, including any errors.

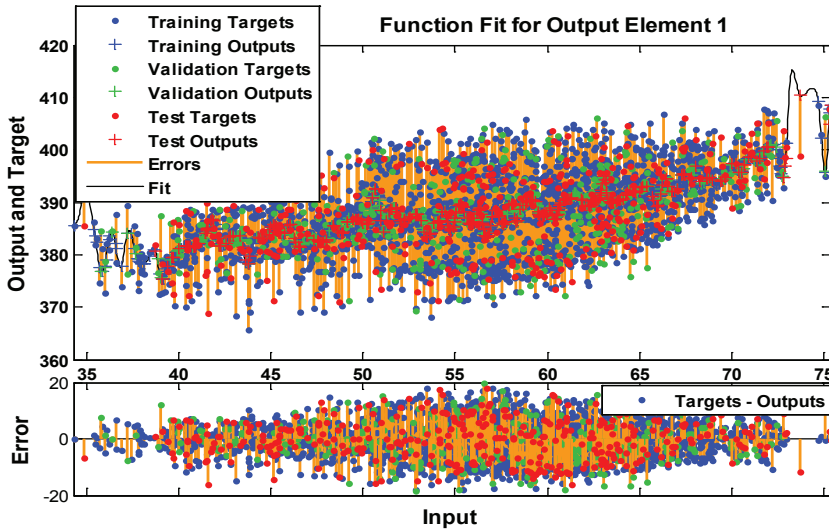


Figure 7: Neural network matching with input-output data, [18]

When the quantity of the sealing steam is known, it is possible to compute thermal power of the sealing steam to be used for the Stirling engine operation and the district heating (condenser). Moreover, the amount of the working gas in the Stirling engine is computed. The data on the working gas quantity is the input data of the third model subprogram (Power output, Figure 5). The above subprogram computes the input and output heat for the Stirling engine operation with the difference representing the engine’s power output. If the power output is multiplied by the engine efficiency rate, the actual power output of the engine is obtained. The actual engine power output constitutes the input data of the fourth subprogram (Stirling engine, Figure 5) that computes the working gas efficiency and thermodynamic properties. The model’s fifth subprogram (Regeneration, Figure 5) computes the Stirling engine’s regeneration rate and efficiency.

#### 4.1 Results of the Stirling engine

In the Stirling engine model analysis, the engine working gas quantity varied according to the sealing steam quantity. At the sealing steam amount of 0.8 kg/s, the engine operates at a minimum working gas quantity. By increasing the sealing steam quantity, the quantity of the working gas in the engine starts to increase. The engine operates at a maximum working gas quantity if the sealing steam flow exceeds 1.6 kg/s. Equation 4.1 describes the pace of change in the working gas quantity with regard to the change in the sealing steam quantity. Figure 8 shows the results of the equation.

$$\begin{aligned}
 m = f(m_s) = & 0,05254 + 0,005581 \cdot \cos(m_s \cdot 1,496) - 0,033 \cdot \sin(m_s \cdot 1,496) - \\
 & 0,01203 \cdot \cos(2 \cdot m_s \cdot 1,496) - 0,02112 \cdot \sin(2 \cdot m_s \cdot 1,498) - \\
 & 0,0103 \cdot \cos(3 \cdot m_s \cdot 1,496) + 0,00169 \cdot \sin(3 \cdot m_s \cdot 1,496) - \\
 & 0,002356 \cdot \cos(4 \cdot m_s \cdot 1,496) + 0,003772 \cdot \sin(4 \cdot m_s \cdot 1,496)
 \end{aligned}
 \tag{4.1}$$

where:  $m_{ss}$  – sealing steam quantity.

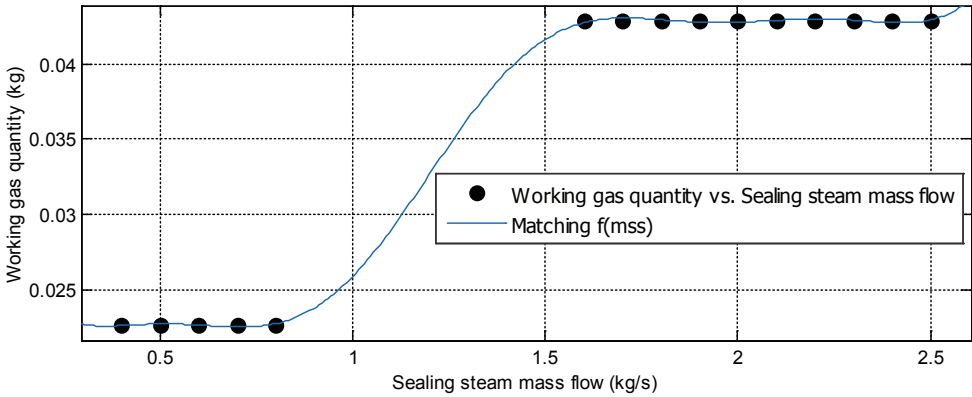


**Figure 8:** Stirling engine working gas quantity vs. sealing steam mass flow, [18]

The model input data includes sinusoidal oscillations of the Stirling engine working gas quantity and temperature, i.e. between the minimum (0.02271 kg/s and 535 K) and maximum value (0.042856 kg/s and 567 K) as shown in Figure 9. The results of the Stirling engine model are plotted for one engine.

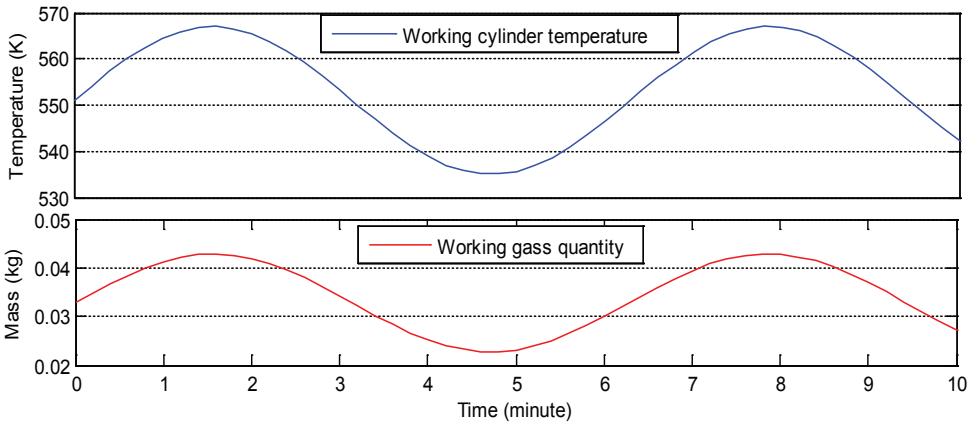


**Figure 9:** Input data of the Stirling engine model, [18]

The results of the input and output heat change model show that between 35 kW and 70 kW of the sealing steam heat (input heat) is used for the Stirling engine’s operation. With the cooling of the Stirling engine’s compression cylinder, the output heat ranges from 20 kW to 35 kW. The engine’s power output is the difference between the input and output heat multiplied by the factor of losses and varies from 13 kW to 32 kW. The results of the Stirling engine’s power output model are shown in Figure 10. The blue area represents the heat needed by the Stirling engine to operate, whereas the red area represents the heat output due to the Stirling engine cooling. The difference is the engine’s power output. As is evident from Figure 10, the engine’s power output increases nonlinearly as the input heat increases, on the basis of which the range of the engine’s rational operation may be established.

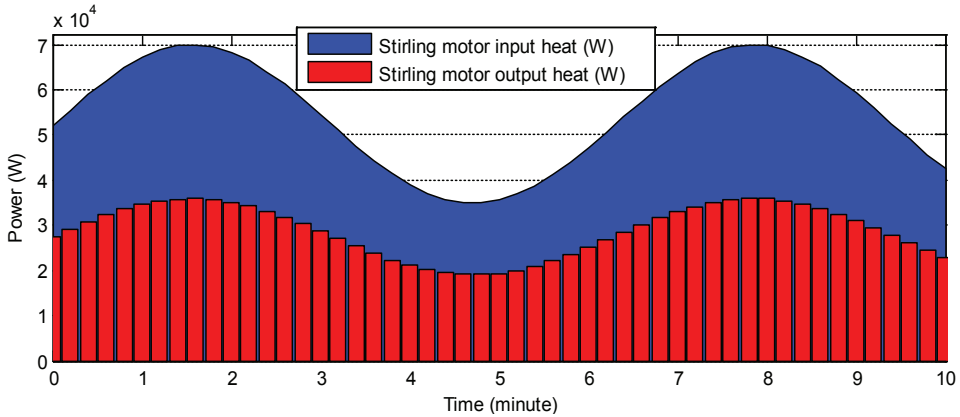


**Figure 10:** Stirling engine input heat, output heat and power, [18]

The results of the regeneration heat model show that regeneration leads to certain losses. The regenerator heat loss is represented by the green area in Figure 11. The blue area represents the regenerator input heat and the red area the regenerator output heat.

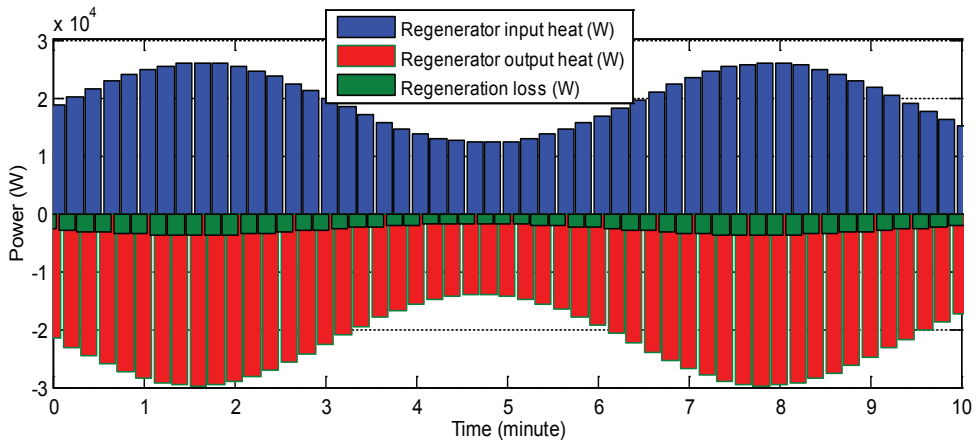


**Figure 11:** Stirling engine regeneration heat, [18]

The results concerning the efficiency reveal an optimum point of the Stirling engine operation, i.e. at a maximum load when the efficiency is the highest. The Stirling engine maximum efficiency using regenerative heat amounts to 46.4% and as low as 33.5% without using regenerative heat. The Stirling engine minimum efficiency is at the minimum engine load. The minimum efficiency using regenerative heat is 45.4% and only 32.8% without using regenerative heat. The Stirling engine's efficiency increases by 12% as a result of the use of the working gas regenerative heat. Figure 12 shows the Stirling engine's efficiency.

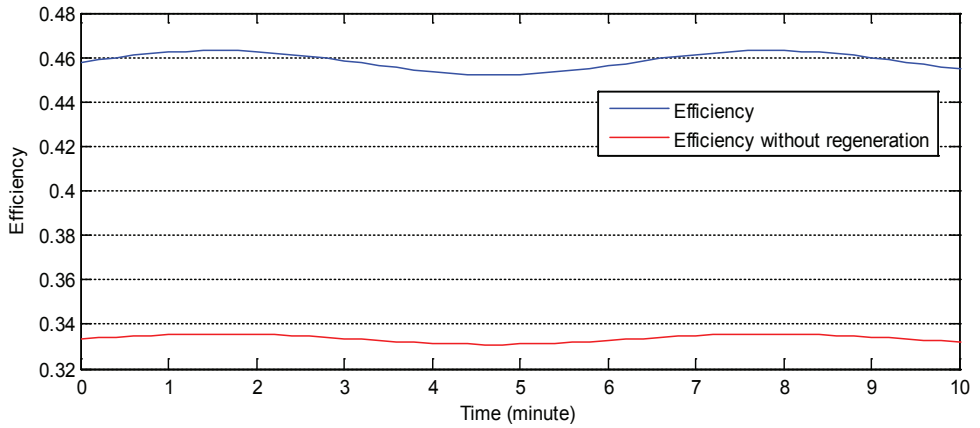


Figure 12: Stirling engine efficiency, [3]

The heat flows, working gas pressure and volume variations at the Stirling engine sinusoidal power oscillation are shown in Figure 13.

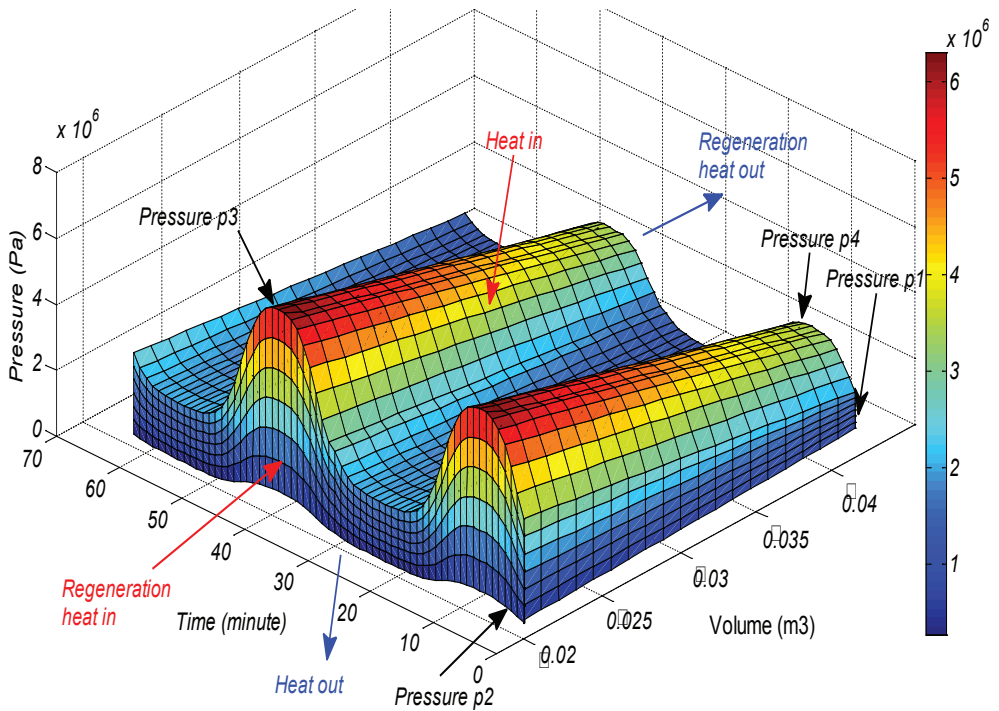
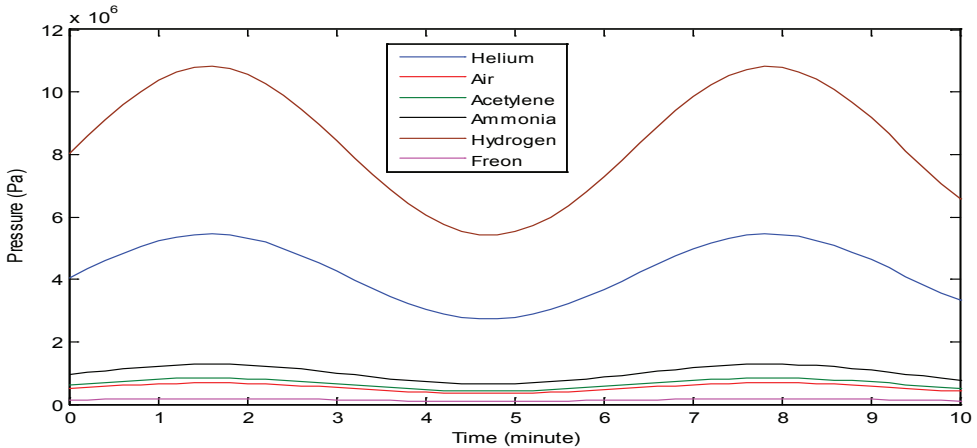


Figure 13: Dynamic  $p - V$  diagram, [18]

Furthermore, simulations of the Stirling engine operating with various working gases were carried out on the existing model. The simulations were carried out by using the gas constants in the model as indicated in Table 1. Figure 14 shows the variation of pressure  $p_3$ , i.e. the maximum Stirling engine pressure.



**Figure 14:** Variation of pressure  $p_3$  at various Stirling engine working gases, [18]

Figure 14 shows that the highest pressure is achieved with hydrogen and the lowest with Freon. The choice of the engine working gas has to be anticipated prior to designing an engine, as the specification of the engine materials should be suitable for the thermal and pressure state. As the working gas pressure state is closely related to the engine's power, the variation in power at different working gases is equivalent to the pressure state. Figure 15 illustrates the Stirling engine's power output variations at different working gases.

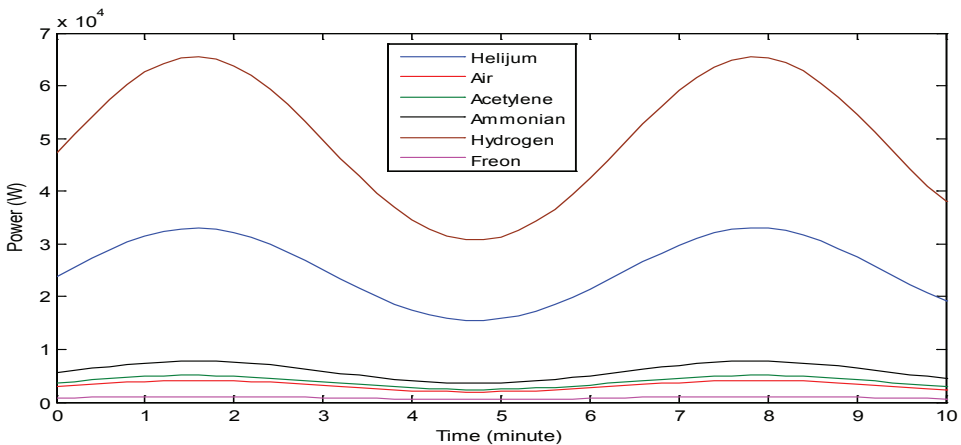


**Figure 15:** Stirling engine power output variations at different working gases, [18]



## 5 CONCLUSION

This paper presents the possibility of using the sealing steam heat of a turbine for heating and power generation. The possibility of using the sealing steam heat that varies in accordance with the energy needs has been indicated. The use of the sealing steam heat for Stirling engines results in electrical energy generation and the application of the engine output heat for the heating of the demineralised supplementary water of a boiler. In the event of an increase in demand for district heating, the sealing steam control system reduces the Stirling engine's power output and increases the heating power. The Stirling engine adapts to the above changes by varying the working gas quantity and adjusting the power to the energy needs.

The installation of Stirling engines into thermal plants is suitable for the use of a smaller amount of waste heat as the issue of overly large engine capacity emerges with larger amounts of waste heat. The above issue is addressed by mounting Stirling engines of a smaller capacity in a successive or a serial-parallel arrangement.

## References

- [1] **S. Toghyani, A. Kasaieian, S. H. Hashemabadi, M. Salimi:** *Multi-objective optimization of GPU3 Stirling engine using third order analysis*, Energy Conversion and Management, 87, (2014), 521–529.
- [2] **J. Ruelas, N. Velazquez, J. Cerezo:** *A mathematical model to develop a Schefflertypesolar concentrator coupled with a Stirling engine*, Appl Energy, 101, (2013), 101, 253–60.
- [3] **S. K. Andersen:** *Numerical simulation of cyclic thermodynamic processes*, PhD Thesis, Department of Mechanical Engineering, Technical University of Denmark, (2006).
- [4] **T. Lia, D. Tanga, Z. Lia, J. Dua, T. Zhou, Y. Jiab:** *Development and test of a Stirling engine driven by waste gases for the micro-CHP system*, Applied Thermal Engineering, 33-34, (2012), 119-123.
- [5] **J. I. Prieto, J. Fano, C. González, M. A. González, R. Diaz:** *Preliminary design of the kinematic Stirling engine using dynamic similarity and quasi-static simulation*, Mechanical Engineering Science, 211, (1997), 229-238.
- [6] **M. Mori, M. Sekavčnik, B. Drobnič:** *Karakteristike stirlingovega motorja*, Univerza v Ljubljani, Fakulteta za strojništvo, (2010) p.p. 3-8.
- [7] **J. L. Salazar, W. L. Chen:** *A computational fluid dynamics study on the heat transfer characteristics of the working cycle of a b-type Stirling engine*, Energy Conversion and Management, 88, (2014), 177–188.
- [8] **H. Karabulut, F. Aksoy, E. Qzturk:** *Thermodynamic analysis of a b type Stirling engine with a displacer driving mechanism by means of a lever*, Renew Energy, 34, (2009), 202–8.
- [9] **W. L. Chen, K. L. Wong, Y. F. Chang:** *A computational fluid dynamics study on the heat transfer characteristics of the working cycle of a low temperature-differential c-type Stirling engine*, Int Journal Heat Mass Transfer, 75, (2014), 145–55.
- [10] **C. H. Cheng, Y. J. Yu:** *Numerical model for predicting thermodynamic cycle and thermal efficiency of a beta-type Stirling engine with rhombic-drive mechanism*, Renew Energy, 35, (2010), 2590–601.

- [11] **U. Stritih, G. Zupan, V. Butala:** *Parametrična analiza Stirlingove sproizvodne enote na biomaso za uporabo v hišni tehniki*, Strojniški vestnik, Journal of Mechanical Engineering, Univerza v Ljubljani, Fakulteta za strojništvo, 2007.
- [12] **F. Sala, C. M. Invernizzi:** *Low temperature Stirling engines pressurised with real gas effects*, Energy, 75, (2014), 225-236.
- [13] **G. Angelino, C. Invernizzi:** *Real gas brayton cycles for organic working fluids*, Proceedings of the Institution of Mechanical Engineers, Part A: Journal of Power and Energy, 215 (1), (2001), 27-38.
- [14] **C. M. Invernizzi:** *Stirling engines using working fluids with strong real gas effects*, Applied Thermal Engineering, 30 (13), (2010), 1703-10.
- [15] **G. Valentia, P. Silvaa, N. Fergnania, G. D. Marcoberardinoa, S. Campanaria, E. Macchia:** *Experimental and numerical study of a micro-cogeneration Stirling engine for residential applications*, Energy Procedia, 45, (2014), 1235-1244.
- [16] **N. C. J. Chen, F. P. Griffin:** *A Review of Stirling Engine Mathematical Models*, Oak Ridge National Laboratory, (1983).
- [17] **N. Parlak, A. Wagner, M. Elsner, H.S. Sohyan:** *Thermodynamic analysis of a gamma type Stirling engine in non-ideal adiabatic conditions*, Renewable Energy, 34, (2009) 266-273
- [18] Matlab: *Computer program*, Simulink, version 2010-a.
- [19] **M. Hooshang, R. A. Moghadam, S. A. Nia, M. T. Masouleh:** *Optimization of Stirling engine design parameters using neural networks*, Renewable Energy, 74, (2015), 855-866.
- [20] **X. S. Zhang:** *Neural networks in optimization*, Springer; 2000.
- [21] **M. K. D. Kiani, B. Ghobadian, T. Tavakoli, A. M. Nikbakht, G. Najafi:** *Application of artificial neural networks for the prediction of performance and exhaust emissions in SI engine using ethanol- gasoline blends*, Energy Convers Manag, (2010), 65-69.
- [22] **Y. O. Özgören, S. Çetinkaya, S. Saridemir, A. Çiçek, F. Kara:** *Predictive modeling of performance of a helium charged Stirling engine using an artificial neural network*, Energy Conversion and Management, 67, (2013), 357–368.

## Nomenclature

$c_v$	Specific heat
$m$	Mass
$p$	Pressure
$P$	Power
$R$	gas constant
$T$	temperature
$V$	Volume
$Q$	Heat
$\sigma$	Regeneration rate
$K$	ratio of specific heats
$\eta$	efficiency
$\pi$	compression ratio

# LOW ENTHALPY SYSTEMS IN GEOTHERMAL ENERGY

## NIZKO ENTALPIJSKI SISTEMI V GEOTERMALNI ENERGIJI

Renato Strojko<sup>✉</sup>

**Keywords:** RES, geothermal energy, low temperature resource, ORC & Kalina processes, Stirling engine

### **Abstract**

Geothermal energy is the most available form of energy and is also weather independent (unlike other types of renewable energy). Furthermore, geothermal energy is present almost everywhere, and it is expected that this energy would have a more important role in the near future. However, not all areas in the world have appropriate geothermal resources, so new technologies are being developed using geothermal resources for generating heat and electricity at low temperatures or enthalpy.

### **Povzetek**

Geotermalna energija je energija, ki je človeštvu najbolj dostopna ter vremensko neodvisna kot druge vrste energije iz družine OVE. Prav tako je količinsko neomejena in pričakovanja so, da se bo ta energija med vsemi najbolj intenzivno širila. Pa vendar niso vsi kraji enako obdarovani z ustreznimi viri geotermalne energije. Zaradi tega se razvijajo nove tehnologije, ki lahko izkoriščajo geotermalne vire za pridobivanje toplote in električne energije z nižjimi temperaturami oz. nižjo entalpijsko vrednostjo.

<sup>✉</sup> Corresponding author: Renato Strojko, BSc. Mech. Eng., Brežice, Tel.: +386 31 358 866,  
E-mail address: [renato.strojko@gmail.com](mailto:renato.strojko@gmail.com)

## 1 INTRODUCTION

Geothermal energy is a renewable energy source that has sparked a great deal of interest, for the production of both electricity and heating, because it is not dependent on the weather. However, geothermal energy is not available to all regions in the world because temperatures in different geothermal resources are not equal, and the possibilities for utilization of them are not the same. The eastern part of our Slovenia is part of the Pannonia region (Pannonia Basin), where geothermal energy can be found more easily than elsewhere; it has thus attracted the attention of scientists, especially from the field of energy technology; they have produced many written expert studies and articles. The central question or problem is almost always the same: is it feasible to build a geothermal power plant for generating electricity? The second question is how to utilize geothermal resources with low temperatures (ca. 40–80° C) for heating and generating electricity.

## 2 GEOTHERMAL ENERGY

Geothermal energy is defined as energy coming from the centre of Earth. Fig. 1 shows temperatures in the Earth.

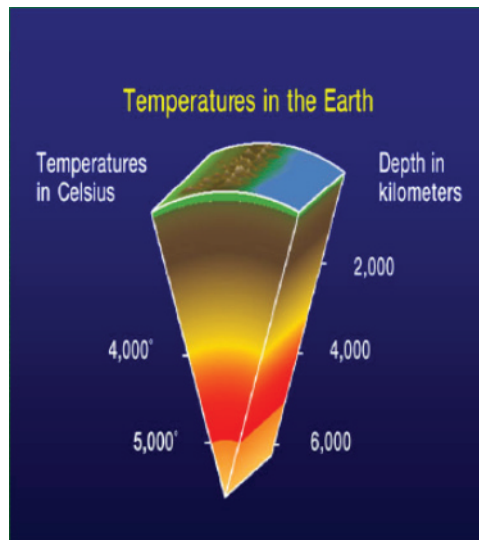


*Figure 1: Temperature in the Earth*

The total flow of heat from the Earth is estimated at  $42 \times 10^{12}$  W (conduction, convection and radiation). Of this figure,  $8 \times 10^{12}$  W come from the crust, which represents only 2% of the total volume of the Earth but is rich in radioactive isotopes;  $32.3 \times 10^{12}$  W comes from the mantle, which represents 82% of the total volume of the Earth, and  $1.7 \times 10^{12}$  W comes from the core, which accounts for 16% of the total volume and contains no radioactive isotopes, [1].

The most important value is the temperature and the quantity of the geothermal resource. On this basis, the kind of geothermal source to be used shall be determined, as can clearly be seen in Lindal diagram (Fig. 2).

Table 1 shows that several types of classification are used; all are based the temperature, and they are distinct according to different geographic areas that provide different conditions for the utilization of geothermal energy. New types of classifications shall be developed according to the latest technologies, all of which have the same goal of obtaining useful heat energy from much lower geothermal resources.

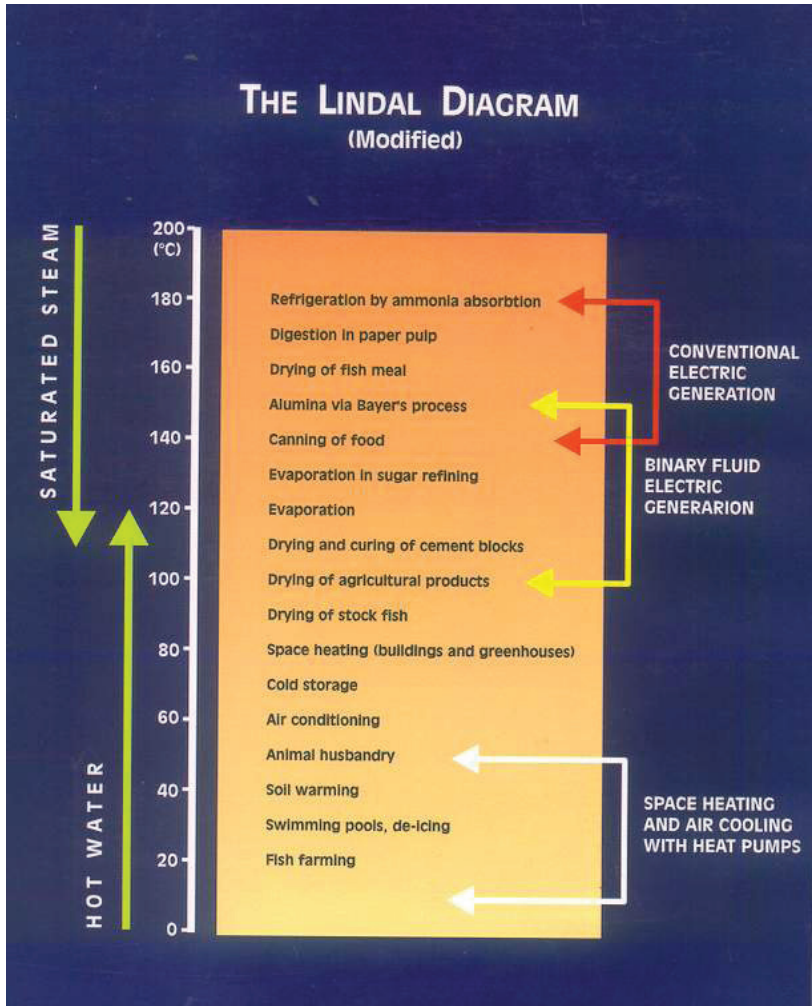


Figure 2: The Lindal diagram

**Table 1:** Different classifications of geothermal resources [1]

	(a)	(b)	(c)	(d)	(e)
Low enthalpy resources	< 90	<125	<100	≤150	≤190
Intermediate enthalpy resources	90-150	125–225	100–200	-	-
High enthalpy resources	>150	>225	>200	>150	>190

Table 1, source: (a) Muffler and Cataldi (1978), (b) Hochstein (1990), (c) Benderitter and Cormy (1990), (d) Nicholson (1993), (e) Axelsson and Gunnlaugsson (2000).

## 2.1 Geothermal energy in Slovenia

Slovenia has suitable conditions for the utilization of geothermal energy. Low temperature resources of geothermal energy dominate (geologically younger structures from the tertiary and quaternary periods); the greatest potential is in the south-eastern part of Slovenia. More than 20 geothermal resources have a constant temperature 20° C. Termal II is the only high temperature aquifer in Slovenia (110°C) at a depth of 2000m. The geologic and tectonic structures of the entire nation are highly complex, and divided into several geothermal regions: the Pannonia reservoir (Banovci spa, Murska sobota and others), the Rogaška-Celje-Šoštanj region (Topolščica, Zreče, Dobrna), the Krško-Brežice region (Šmarješke toplice, Čateške toplice, Bušeća vas), the Planinsko-Laško-Zagorje region (Medijske toplice, Laško, Rimske toplice, Podčetrtek), the Ljubljana basin (Ljubljana moor, Podpeč, Vrhnika, temperature about 18-30 °C) [2].

In Slovenia, geothermal water is divided according to:

- Temperatures under 25° C: convenient for heat pumps, which can utilize such energy
- Temperatures between 25–90° C: convenient for direct utilization. The biggest aquifer is Termal I in Murska Sobota. Around 400 GWh heat energy is available.
- Temperatures greater than 90°C; The Termal II aquifer is the only one, and it is suitable for generating heat and electricity
- As can be seen in Fig. 3, low temperature geothermal resources dominate in Slovenia. These resources that are interesting from the perspective of energy production.

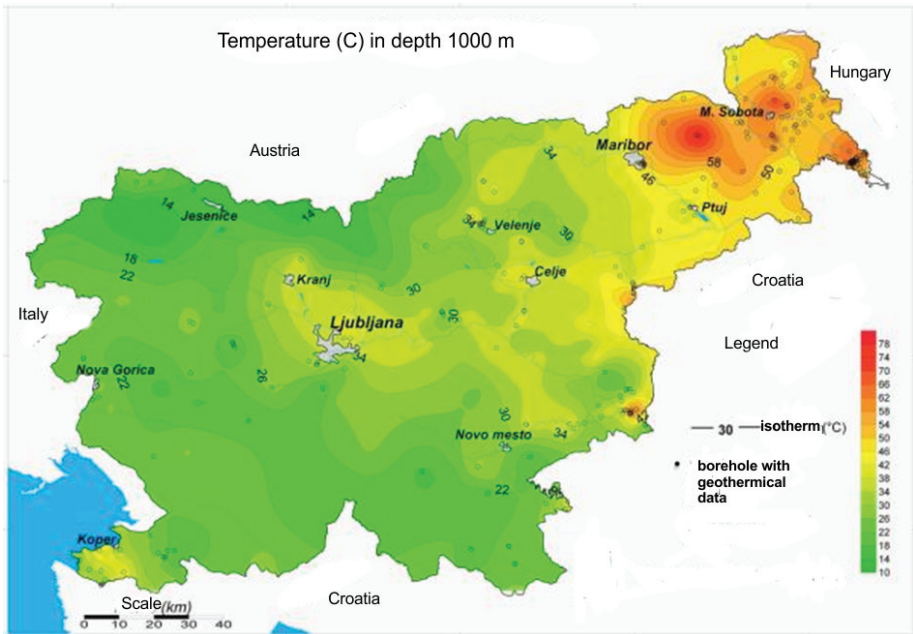


**Figure 3:** Temperatures of geothermal resources in Slovenia

A typical geothermal resource is Mostec near Čatež, [3], classified as a low temperature or low enthalpy resource, with a temperature of 61 °C, a flow of 40 l/s and maximum available power of 7.8 MW<sub>t</sub>. This resource has been repeatedly studied and all have reached the same conclusion that the resource is under-utilized and inappropriately maintained. A quick calculation shows that for 60 houses in the village of Mostec a mere 1.8 MW is needed. Energy experts are alarmed by this situation; the owner of Mostec resource is the state. Furthermore, it was determined that a nearby health spa where still hot once-used water with temperatures of 30-35° C runs into the sewer system, [2].



**Figure 4:** Abandoned geothermal resource in Mostec



At the same time, Slovenia states in its documents renewable energy sources (AN OVE 2012-2020) [4] that there will be no electricity generated from geothermal power plants. Nevertheless, significant progress has been made in ground (geothermal) source heat power or GSHP. To the middle of 2010, almost 4,410 GSHP units had been installed. It may be expected that up to 1,000 units shall be installed annually in the next five years.

From a technical point of view, the obvious question is what else can low temperature geothermal sources teach other non-technical people about suitable utilization of available resources. Low temperature geothermal resources are appropriate for generating heat and electricity with so-called binary systems or cycles, which are well known in the energy production field, but less so by the general public.

## 2.2 Systems for generating electricity

Classification of all geothermal systems that can generate electricity:

- high-temperature resource (more than 150° C) – dry steam
- middle-temperature resource (between 90 and 150° C) – flash steam
- low-temperature resource (T under 90° C) – binary cycle

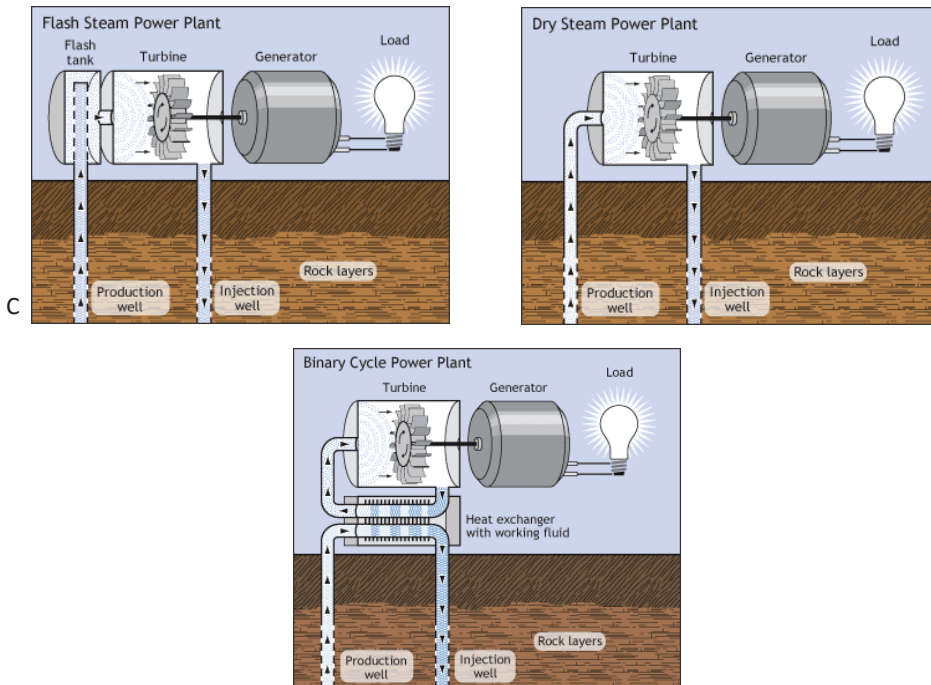


**Figure 5:** Systems for generating electricity

The latest technology is called EGS (Enhanced geothermal system).



## 2.3 Systems for generating heat and electricity from low enthalpy resources

Very recently major technological progress has been made and the possibility of generating heat and electricity from low enthalpy resources has now become a reality. In Fig. 6, it is shown that appropriate systems for using low enthalpy resources are the ORC and Kalina processes. Furthermore, some good results have been brought about with a new Stirling engine concept especially designed for geothermal resources.

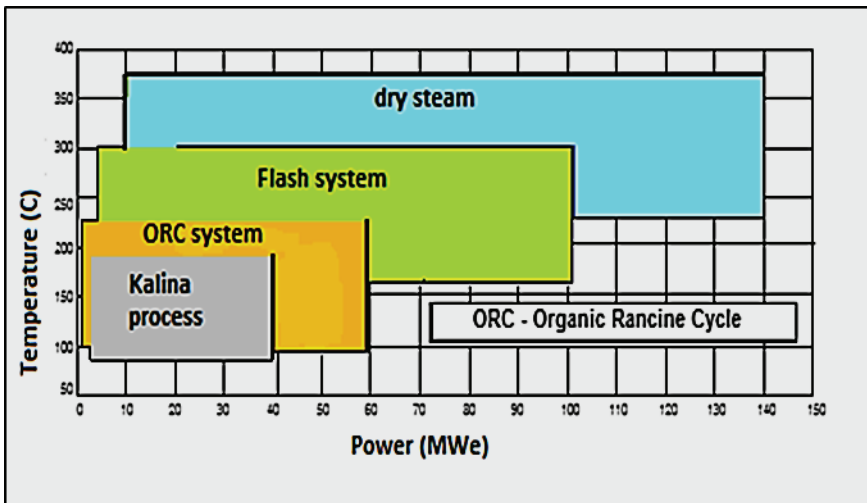
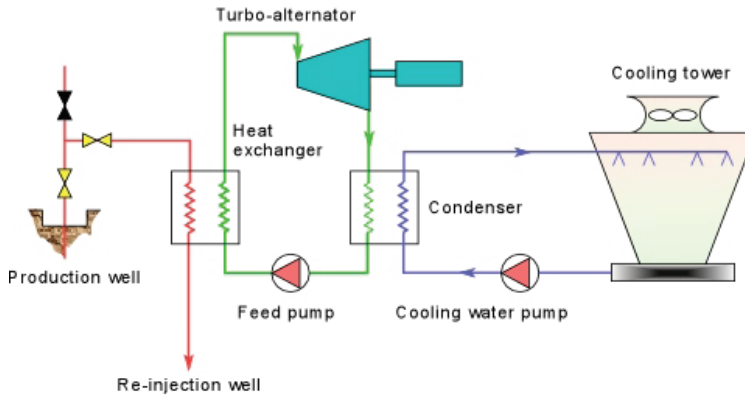


Figure 6: Using of geothermal energy according to the temperature of geothermal resource, [5]

### 2.3.1 Binary plants – ORC cycle

Generating electricity from low-to-medium temperature geothermal fluids and from the waste hot water coming from the separators in water-dominated geothermal fields has made considerable progress since improvements have been made in binary fluid technology. The *binary plants* utilize a secondary working fluid, usually an organic fluid (typically n-pentane) that has a low boiling point and high vapour pressure at low temperatures in comparison to steam. The secondary fluid (Freon, Isobutene, Isopentane, R-115, R-717, R-22, R 114, etc.) is operated through a conventional Rankine cycle (ORC), [1]; the geothermal fluid yields heat to the secondary fluid through heat exchangers, in which this fluid is heated and vaporises; the vapour produced drives a standard axial flow turbine, is then cooled and condensed, and the cycle begins again (Fig. 7). According to the latest research, binary plants can function even with temperature sources at 57°C (the temperature of the Mostec resource).



**Figure 7:** Binary system, [1]

Binary plants are usually constructed in small modular units of a few hundred kW<sub>e</sub> to a few MW<sub>e</sub> capacity. These units can then be linked up to create power-plants of a few tens of megawatts. Their cost depends on a number of factors, but particularly on the temperature of the geothermal fluid produced, which influences the size of the turbine, heat exchangers, and cooling system. The total size of the plant has little effect on the exact cost, as a series of standard modular units is joined together to obtain larger capacities.

### 2.3.2 Kalina process

A new binary system, the Kalina cycle, which utilizes a water-ammonia mixture as working fluid, was developed in the 1990s. The working fluid is expanded, in super-heated conditions, through the high-pressure turbine and then re-heated before entering the low-pressure turbine. After the second expansion, the saturated vapour moves through a recuperative boiler before being condensed in a water-cooled condenser. The Kalina cycle (Fig.8) is more efficient than existing geothermal ORC binary power plants, but is of a more complex design, [1].

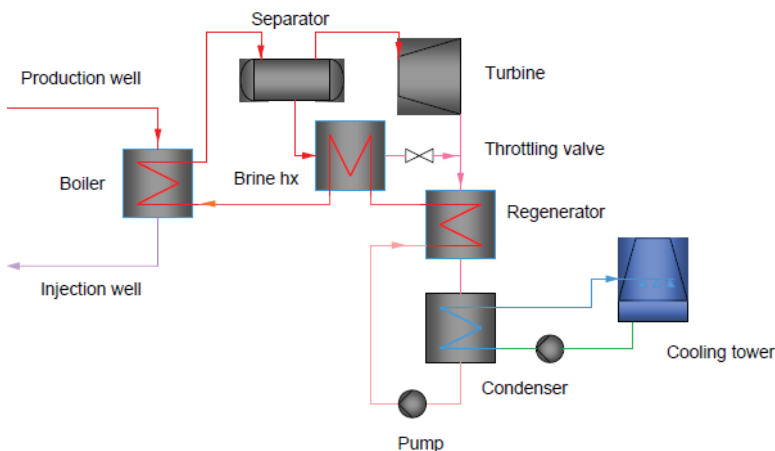


**Figure 8:** Kalina process

Small mobile plants, conventional or not, can not only reduce the risk inherent to drilling new wells, but, more importantly, they can help in meeting the energy requirements of isolated areas. The standard of living of many communities could be considerably improved were they able to draw on local sources of energy. Electricity could facilitate many apparently ordinary, but critical operations, such as pumping water for irrigation, freezing fruit and vegetables for longer conservation, etc.

Such ORC, including Kalina processes, still need temperatures of geothermal resources near the boiling point of water; at this moment, energy cannot be generated from lower temperatures of geothermal resources.

### **2.3.3 Stirling engine in geothermal energy**

The low temperature potential of some geothermal reservoirs is their major disadvantage when it comes to power generation, since the abovementioned processes require reheated steam for their operation. Therefore, the Stirling cycle seems to be a better and more practical solution resulting in considerably higher efficiency, because it is thermodynamically equivalent to the optimum Carnot's cycle. The development of a Stirling engine with flat plate heat exchangers (Stirling-Kolin engine) has shown that the low temperature geothermal reservoirs may also be successfully used for the conversion of heat into mechanical work or electric energy. Hot water from the well circulates through a number of flat boxes connected with a crankshaft driven by a generator. After its heat is transferred to the plant, the cooled water is returned into the reservoir using an injection pump. Additionally, the geothermal plant using the Stirling cycle has considerable technical and economic advantages in comparison to the classic Clausius-Rankine process because there is no evaporator, condenser, feed water pump or numerous other associated elements [6].

All the thermodynamic processes for the conversion of heat into mechanical work, and in particular for the low temperature resources, are dependent upon the ambient temperature. Each heat engine works better during the winter than during the summer time.

The key feature of this engine design that would make it attractive to potential buyers is its ability to run on a variety of low grade heat sources that are potentially free; however, for it to be successful in the marketplace, it must be very cost competitive as an outright purchase. If a small version (1-4 kW output) was able to be produced cheap enough, then it could potentially find its way into applications such as off-grid domestic power generation [7].

## **3 CONCLUSIONS**

Energy is becoming very expensive and also strategic, for each family budget, for each state, and for our currently united Europe. Its institutions and chambers have prescribed very detailed plans with actions due to energy saving and energy efficiency in all economic fields. According to the new regulations, buildings must have efficient heat envelopes, which is basic for using low-power generator. For this reason, a strong trend for the utilization of such generators has begun. An action plan called "Each J counts" has begun.

In an expert article written by geologists, [8], it was again concluded that theoretical possibilities for geothermal power plants in Slovenia exist but in order to start serious and detailed discussion

about such plants, more research has to be done. Areas with geothermal energy have been very well researched, so new geothermal resources are not expected to be found.

For the research of geothermal resources, grants should be given to the laboratories, institutes, universities for the basic task of developing the above-described systems.

Organizing and demonstrating the latest technologies and experiences in using of low enthalpy geothermal resources is the next step forward. It should be followed by different types of subsidies to increase the number of investors using small geothermal power plants. These plants in the first phase still have to be developed and tested and then placed into operation.

The Mostec geothermal resource is to be used for generating electricity. From the technical point of view, there is no problem, but economic questions regarding such a solution remain. How much the cost of electricity from such a resource would be cannot be exactly determined in advance. Naturally, the cost of electricity would be a key factor in any economic analysis and decisions for investment. Currently, Slovenia lacks investors for such an investment.

The progress of binary systems shall continue by developing new material and working fluids. The temperature of geothermal resources needed for first phase (i.e. for thermal water from for heating and vaporizing of secondary working fluid) would be lower. It could be expected that the possibilities for generating heat and electricity would be better, with temperatures from 80° C to 40° C or even less.

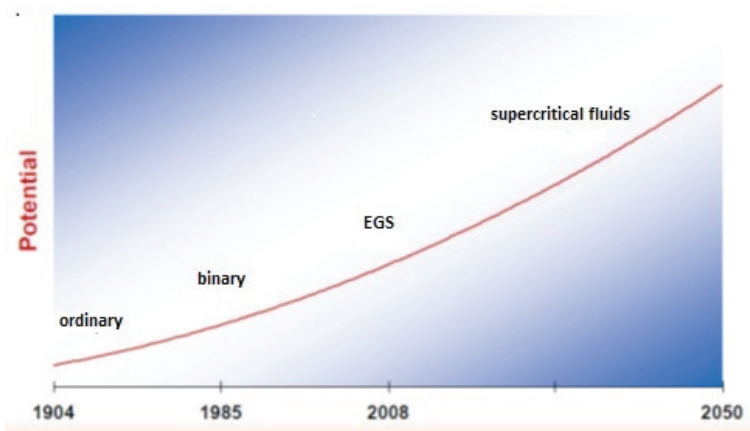


**Figure 9:** Potential of geothermal energy

The transformation of geothermal heat into mechanical or electrical work is generally discussed mostly for the relatively large scale of several thousands of kW. In contrast, the small range of power of a few kW is often neglected in the case of geothermal resources. Nevertheless, only one kW power could be quite sufficient to drive a circulation pump for a very large quantity of geothermal water in very different applications. Practical examples could be space heating, various technological processes using moderate temperatures, and other similar systems.

All these examples require a significant amount of heat, but relatively small pumps to circulate hot geothermal water. For the time being, low temperature difference Stirling motors, driven by hot

water, are not available in large power units. However, due to the promising contemporary development of geothermal Stirling engines, ever-growing power units will most likely soon be available to cover increasing energy needs as well.

However, a new concept of Stirling motor is being developed that is able to use low temperature geothermal resources; it is currently entering production.

## **References**

- [1] **M.H. Dickson, M. Fanelli:** *What is geothermal energy*, Istituto di Geoscienze e Georisorse, CNR, Pisa, Italy, February 2004
- [2] Tehnocenter Univerze v Mariboru: *Novelacija študije energetskega koncepta v občini Brežice*; Občina Brežice, Maribor, junij 2009
- [3] **E. Sečen:** *Geotermalna energija je in ni*, Dnevnik, 26.april 2010
- [4] **MG RS:** *Akcijski načrt za obnovljive vire energije za obdobje 2010-2020 (AN OVE) Slovenija*, Ljubljana, julij 2010
- [5] **B. Grobovšek:** *izkoriščanje geotermalne energije za proizvodnjo električne energije*, ZRMK
- [6] **I. Kolin, S. Koscak-Kolin, M. Golub:** *Geothermal electricity production by means of the low temperature difference stirling engine*, World Geothermal Congress 2000, Tohoku Japan, May-June, 2000
- [7] **C.C. Llyod,** *A low temperature differential stirling engine for power generation*, University of Canterbury, 2009
- [8] **D. Rajver, A. Lapanje, N. Rman,** *Možnosti proizvodnje elektrike iz geotermalne energije v Sloveniji v naslednjem desetletju*, GEOLOGIJA 55/1, 117-140, Ljubljana 2012



# REVIEW OF ENERGY REGULATIONS ON SOLAR ENERGY (PV) IN SLOVENIA AND AUSTRIA

## PREGLED ENERGETSKE REGULATIVE ZA SONČNO ENERGIJO (PV) V SLOVENIJI IN AVSTRIJI

Franjo Pranjič<sup>✉</sup>

**Keywords:** PV-photovoltaics, Action Plan for Renewable Energy and Energy Efficiency

### **Abstract**

This paper describes the regulation of solar energy (PV) in Slovenia and Austria, what parties provides support and incentives and how, who is eligible and who is not. All the principal documents regulating this area in Slovenia and Austria are listed. The present value of support for PV installations and a comparison of support schemes are also presented.

### **Povzetek**

Članek opisuje energetske regulative na področju sončne energije (PV) v Sloveniji in Avstriji, kdo in kako zagotavlja podporo in spodbude, kdo je upravičen in kdo ni. Opisani so glavni dokumenti, ki urejajo to področje v Sloveniji in Avstriji. V članku so prav tako predstavljene sedanje višine podpor za fotonapetostne naprave ter primerjava podpornih shem.

<sup>✉</sup> Corresponding author: Franjo Pranjič, Tel.: +386 3 777 0402, Mailing address: University of Maribor, Faculty of Energy Technology, Koroška cesta 62a, 3320 Velenje

## 1 INTRODUCTION

The Kyoto Protocol 2020 compels the countries that signed it to reach a defined share of energy production from renewable energy sources (RES) and a defined reduction of emissions in each country. For that purpose, there are different regulations and initiatives to support energy production from renewable energy sources. This article presents and compares the support schemes in Slovenia and Austria for solar energy, i.e. photovoltaic installations (PVs).

## 2 SUPPORT SCHEMES IN SLOVENIA

Borzen, d.o.o. is a Slovenian power market operator. Its principal activity is the implementation of public service obligations relating to the organization of the electricity market, which includes the organization of the electricity market and the activities of the Centre for RES/CHP Support.

In Slovenia, electricity generated from renewable energy is supported mainly via a feed-in tariff and a premium tariff. Certain producers (“qualified producers”) of electricity from renewable sources may choose between a guaranteed feed-in tariff and a bonus (“premium”) in addition to the free market price for electricity. Furthermore, public calls for subsidy applications are organized, and loans are provided for projects in the field of renewable energy, [1].

### 2.1 Centre for RES/CHP

The centre administers the electricity feed-in support scheme for RES (renewable energy source) and CHP (high-efficiency cogeneration) power plants.

The feed-in support scheme is a tool to subsidize and thus advance the usage of renewable technologies for the production of electricity. There are currently roughly 3700 power plants included in the scheme, predominantly hydro and PV. The total installed capacity is about 500 MW.

The feed-in scheme, as well as other tools, is financed through dedicated add-on charges on the network fee bills of all users of electricity in Slovenia.

Power plant owners have the option of choosing between two types of support:

- “guaranteed purchase”, whereby CP takes over the electricity from the power plant and sells it to the market (the producer is thus included in the special balance group operated by CP)
- “operating premium”, whereby the producer sells its energy on the market while CP only pays a premium as a difference between the full (“guaranteed purchase”) price and the market price, which is determined *ex ante* on a yearly level, also based on plant type.

Producers with power plants of installed capacity over 1 MW can only receive the “operating premium” support.

The feed-in system is based on guarantees of origin. All producers included in the scheme must issue and transfer to CP guarantees of origin as proof of RES / CHP production.

Based on the Slovenian Energy Law, the centre carries out also the following tasks, related to:

- guaranteeing the security of electricity supply based on the usage of domestic primary energy sources,



- ensuring an adequate level of installed capacity for the production of electricity and programmes for efficient use and saving of electricity, [1].

## 2.2 Means of support in Slovenia

Means of support in Slovenia are:

- Feed-in tariff,
- Loan (Eko Fund),
- Premium tariff,
- Subsidy scheme of the Ministry for Infrastructure and Spatial Planning.

### 2.2.1 Feed-in tariff

Regarding the feed-in tariff, producers of electricity from renewable sources (qualified producers) using plants of up to 1 MW may decide that they would like their electricity to be purchased at a fixed price.

The operators of renewable energy plants may sell their electricity to the Slovenian power market operator Borzen at a “uniform annual price”, i.e. the feed-in tariff (alternatively, they can opt for a premium tariff). This guaranteed price applies only to plants whose capacity does not exceed 1 MW, [2].

Producers of electricity from renewable sources are eligible only if they have a valid declaration for the production device. All producers of renewable energy are usually deemed to have the declaration as long as they use any of the listed RES technologies, [2].

The tariff rates are calculated on a monthly basis due to the change in the regression mechanism, which implies a monthly degression of the Reference Costs by 2%.

**Table 1: Slovenian feed-in tariffs for June 2014**

Building-mounted PV installations:	Other PV installations:
up to 50 kWp: €ct 10.428 per kWh	up to 50 kWp: €ct 9.798 per kWh
up to 1 MWp: €ct 9.536 per kWh	up to 1 MWp: €ct 9.026 per kWh
up to 5 MWp: €ct 7.913 per kWh	up to 5 MWp: €ct 7.277 per kWh

For each following month, the tariff is reduced by 2%. Building-mounted PV installations up to 5 kWp (which are connected behind the end user’s meter) are entitled to an additional 5% of the reference costs.

The entitled persons are those plant operators that have a valid award decision from the Energy Agency and a declaration for their RES-E power plant, [3].

## PROCEDURE

The Energy Agency issues a public call by October each year, which is open to investors with RES and CHP power plants, to submit their projects for which they wish to receive support in the following year. [2]

Projects are selected on the basis of the following criteria:

- the available funds for the support for the next year set by the Government on the basis of the adopted annual energy balance sheets (EZ-1),
- compliance of the project with the goals of the NREAP and the goals set in the yearly energy balance sheets,
- the estimated level of guarantee of acquiring the necessary funds from the European Union funds,
- the proposed price (by the producer) of the electricity production costs that will be subject to the received support (EZ-1).

The Energy Agency submits its decision to grant support to the plant operator, Borzen, and the plant operator shall then conclude a contract on the purchase of electricity, based on the decision.

The government may, in order to ensure the sustainability of the support scheme, limit the annual installed power of installations receiving support for specific technologies and energy sources, if the share of installed generating plants exceeds the yearly planned volume in the adopted Action Plan for Renewable Energy and Energy Efficiency, [2].

Eligibility period is no more than 15 years.

### 2.2.2 Loan (Eko Fund)

The Environmental Fund of the Republic of Slovenia (Eko sklad) awards low-interest loans to renewable energy projects through tendering (Terms and Conditions of the Eco Fund). At the moment (June 2014), there are two public calls for loans in the field of RES-E. The current calls for applications subsidise the reconstruction and renovation of renewable energy plants. They apply to municipalities, enterprises, sole traders and other legal entities in the Republic of Slovenia as well as residents.

Solar energy is eligible for this support with the exception of Industrial Ground-mounted PV Systems.

The amount of credit must be determined in line with the provisions of Terms and Conditions of the Eco Fund. According to these provisions, the amount of credit depends on the following factors:

- the amount of eligible costs,
- the type of investment,
- the evaluation of the environmental criteria,
- the credit rating of the eligible party and the debt insurance,
- the total budget available for a specific call, as defined in the public call document,
- the relevant state aid and “de minimis” limits.

The calls currently open provide a total of €24 million for municipalities, enterprises, and other legal entities and €8 million for residents. For legal entities, the maximum loan size is €2 million, the minimum loan is €23,000. For private individuals (residents), the loan amount ranges from €1,500 to €20,000 or €40,000 in special circumstances.

The maximum credit period is 15 years for legal entities and 10 years for private individuals. The credit period may, however, be extended for legal entities if they prove that such an extension is reasonable.

The minimum interest rate for legal entities and residents is the three-month EURIBOR rate plus 1.5 percentage points.

All public or private legal entities and natural persons whose place of residence, branch or head office is in Slovenia are eligible.

#### PROCEDURE

- Application:

Applicants submit their applications to the Environmental Fund of the Republic of Slovenia (Eco Fund), [4].

- Loan award:

The decision on the award of a loan is based on the general provisions of administrative law and the procedure set out in the Rules on the Allocation of the Budget According to the terms of the current calls, the Fund decides on whether or not a loan will be granted and informs the applicant of this decision within a period of 90 days.

- Loan contract for private individuals.

Private individuals must enter into a loan contract with the lending institution within 10 days of the loan being granted. The total amount of credit is paid either as a lump sum or in two instalments by the lending bank. The first instalment is 40% of the total loan amount and is paid within five days of the loan contract being signed. The remaining 60% are paid within five working days of the applicant submitting evidence that the investment has been made.

- Loan contract for legal entities.

Except for municipalities, applicants must enter into a loan contract within six months of the date on which the loan is granted. Municipalities must sign the contract within nine months of the being is granted.

### **2.2.3 Premium tariff**

Operators of renewable energy plants with an installed capacity of up to 1 MW may choose to sell their electricity directly on the market instead of receiving the guaranteed purchase price (feed-in tariff). In this case, they will receive a so-called “operational support” (i.e. a premium tariff). Power plants with a capacity of more than 1 and less than 10 MW (with the exception of CHP plants with capacity of up to 20 MW and wind power plants up to 50 MW) may only opt for this support scheme, [2,3].

Producers of electricity from renewable sources are eligible only if they have a valid declaration for their plant and an award decision from the Energy Agency. In principle, all RES plants receive the declaration.

The premium tariff is paid for the net amount of generated electricity that the producers themselves sell on the market or use for their own consumption, provided that the production costs of this energy are higher than the market price.

The amount of the premium tariff is the difference between the reference costs of electricity for each RES technology and the market price of electricity multiplied by a so-called “B factor”, which leads to following formula:

$$\text{Premium} = \text{RC (Reference costs)} - \text{MP (Market Price for electricity)} * \text{B factor} \quad (2.1)$$

In 2014, the reference market price of electricity amounts to €ct 4.331 per kWh.

The tariff rates are calculated on a monthly basis due to a change in the regression mechanism, which implies a monthly regression of the RC by 2%.

**Table 2: Slovenian reference cost rates for June 2014**

Building-mounted	RC (€ct per kWh)	B factor	Other PV	RC (€ct per kWh)	B factor
up to 50 kW	10.428	0.88	up to 50 kW	9.798	0.88
up to 1 MW	9.536	0.88	up to 1 MW	9.536	0.88
up to 10 MW	7.913	0.91	up to 10 MW	7.277	0.91
up to 125 MW	7.042	1	up to 125 MW	6.756	1

The entitled recipients are those plant operators that have a valid award decision from the Energy Agency and a declaration for their RES plant.

#### PROCEDURE

The Energy Agency issues a public call by October each year, which is open to investors with RES and CHP power plants, to submit their projects for which they wish to receive support in the following year.

Projects are selected on the basis of the following criteria:

- the available funds for the support for the next year set by the government on the basis of the adopted annual energy balance sheets,
- compliance of the project with the goals of the NREAP and the goals set in the yearly energy balance sheets,
- the estimated level of guarantee of acquiring the necessary funds from the European Union funds,
- the proposed price (by the producer) of the electricity production costs that will be subject to the received support.

The eligibility period limit is set to a maximum of 15 years.

## 2.2.4 Subsidy scheme of the Ministry for Infrastructure and Spatial Planning

The Ministry for Infrastructure and Spatial Planning of the Republic of Slovenia awards subsidies, state aid (regional aid, aid for small and medium enterprises) and “de minimis” aid. For investment projects, these are awarded through tendering.

The tender document sets out the technologies to be supported, the tendering process, and how the subsidy is paid. Tenders are launched on a regular basis (ca. 2-3 Tenders per month). Currently, all tenders that would support investments in RES-E projects are awarded via state-owned energy companies.

The subsidies, state aid and “de minimis” aid are intended to cover some of the costs related to the use of renewable energy instead of traditional energy sources. Please note the following important information:

- Subsidies are subject to a maximum of 50% of the eligible costs of an investment project; state aid and “de minimis” aid grants are subject to a maximum of 30%. Exceptional projects may be awarded 40/50% of the costs.
- The maximum grant is defined in each particular tender.

Certain grants are subject to a maximum (e.g. €50,000 for state aid and €200,000 / €100,000 for “de minimis” aid). In these cases, a report must be submitted to the Ministry of Finance.

The following entities are eligible for grants:

- For consulting services and projects in the fields of energy efficiency, renewable energy and CHP: local communities which have adopted the local energy concept.
- Households.
- For advisory services and investment projects in the fields of energy efficiency, renewable energy and CHP, all non-commercial public funds, public agencies, institutions, foundations and associations, registered churches and other religious communities.

### PROCEDURE

- Application

The tender document specifies the requirements for support. Applicants must submit a signed application form that comes with the tender document a full investment and financial plan and evidence that they have invested a certain amount of their equity in the project.

- Award

Applications will be examined by a commission from the ministry or by the financier, according to the procedure set out in ZUP, [5].

- Subsidy contract

The applicant shall sign a subsidy contract with the authority responsible for the payment of the subsidy (the Ministry for Infrastructure and Spatial Planning).

### 2.2.5 Statutory provisions

- ZUP (Zakon o splošnem upravnem postopku - neuradno prečiščeno besedilo, PisRS z dne 22.02.2010 - Administrative Procedures Act)
- Energy Act (Energetski zakon)
- RS 37/2009 (Uredba o podporah električni energiji, proizvedeni iz obnovljivih virov energije – Uradni list RS, 37/2009 - Decree on the Support for Electricity Generated from Renewable Energy Sources)
- RS 8/2009 (Uredba o izdaji deklaracij za proizvodne naprave in potrdil o izvoru električne energije – Uradni list RS 8/2009 - Decree on the Issue of Certificates for Energy Generation Plants)
- RS 89/2008 (Pravilnik o spodbujanju učinkovite rabe energije in rabe obnovljivih virov energije - Uradni list RS, 89/2008 - Resolution on Promoting Energy Efficiency and the Use of Renewable Energy)
- RS 57/2004 (Resolucija o Nacionalnem energetskem programu - Uradni list, 57/2004 - Resolution on the National Energy Programme)
- RS 50/2007 (Pravilnik o postopkih za izvrševanje proračuna Republike Slovenije - Uradni list, 50/2007 - Regulation on the Allocation of the Budget)
- Statute of the Eco Fund (Akt o ustanovitvi Eko sklada, Slovenskega okoljskega javnega sklada – Uradni list RS 112/2009 - Act on Establishing the Eco Fund – the Slovenian Environmental public Fund)
- Terms and Conditions of the Eco Fund (Splošni pogoji poslovanja za spodbujanje razvoja na področju varstva okolja – Uradni list RS 117/2005 – General terms and conditions for promoting the development in the field of environmental protection)
- Call No. 49OB13 (Javni poziv za kreditiranje okoljskih naložb občanov 47OB12 - Call for applications by the Eco Fund for environmental investments by citizens)
- Call No. 50PO13 (Javni poziv za kreditiranje okoljskih naložb 50PO13 - Call for applications by the Eco Fund for environmental projects by legal entities)
- RS 2/2009 (Uredba o načinu določanja in obračunavanja prispevka za zagotavljanje podpor proizvodnji električne energije v soproizvodnji z visokim izkoristkom in iz obnovljivih virov energije – Uradni list RS 2/09 - Decree on the Calculation and Payment of the Support for High-Efficiency CHP Generation and Renewable Energy Generation)

### 3 SUPPORT SCHEMES IN AUSTRIA

In Austria, electricity from renewable sources is mainly supported through a feed-in tariff. Furthermore, the construction of PV installations on buildings and small or medium-sized hydro-electric power stations is supported through subsidies, [6].

Support schemes:

- Feed-in tariff.

In Austria, electricity from renewable sources is supported mainly through a feed-in tariff, which is set out in the ÖSG 2012 and the regulations related thereto. The operators of renewable energy plants are entitled against the government purchasing agency, the so-called Ökostromabwicklungsstelle (hereinafter: “Clearing and Settlement Agency”), to the conclusion of a contract on the purchase of the electricity they produce (“obligation to enter into a contract”).

- Subsidy II.

Additionally to the feed-in tariff, an investment subsidy is granted for PV installations exceeding 5 kW on buildings.

- Subsidy III.

Furthermore, subsidies are granted for small PV installations with a maximum capacity of 5 kW.

#### 3.1 Means of support in Austria

- Feed-in tariff (ÖSG 2012)
- Subsidy II (Investment Subsidy for PV)
- Subsidy III (Investment subsidy for small PV)

##### 3.1.1 Feed-in tariff (ÖSG 2012)

Electricity from renewable sources is supported mainly through a feed-in tariff. The operators of renewable energy plants are entitled to the conclusion of a contract with a government purchasing agency, the Clearing and Settlement Agency, on the purchase of and payment for electricity as long as funds are available, [7].

The feed-in tariffs for the different renewable technologies are stipulated annually through a resolution of the Minister of Economy, Family and Youth, [7].

Solar energy is eligible under the following condition: the installation’s capacity shall exceed 5 kWp, PV installations on roof-tops and facades with capacities over 5 kWp, up to 350 kWp, if application submitted and contract concluded until the end of 2014: €ct 12.5 per kWh. Other PV installations with capacities over 5 kWp, up to 350 kWp, if application submitted and contract concluded until the end of 2014: €ct 10.00 per kWh. [7]

- Entitled party

The persons entitled to the tariff are the operators of renewable energy plants. In order for a plant operator to be entitled to the tariff, the plant he claims tariff for must be licensed as a “green electricity plant” (Ökostromanlage). Plants are licensed by the governor.

- Obligated party

The Clearing and Settlement Agency, which is obliged to the purchase of all electricity generated from renewable energy sources as long as funds are available. The Clearing and Settlement Agency is a private enterprise that has a state licence and is responsible for the purchase and sale of electricity from renewable sources within the territory of Austria.

- Electricity trader

The second party obliged to satisfy a claim for the feed-in tariff are the electricity traders, who are obliged to purchase the quantities of electricity assigned to them by the Clearing and Settlement Agency at the transfer price set by law.

## PROCEDURE

The Clearing and Settlement Agency is obliged to purchase electricity from all renewable sources regardless of the generation technology used, under the following conditions:

- There are still funds available for the current year.
- The plant in question has been commissioned, and the contract with the Clearing and Settlement Agency has been concluded.
- The producer in question is obliged to supply green electricity for at least twelve calendar months.
- The producer is obliged to join the eco-balance group.
- The responsible authority is the Ministry of Economy, Family and Youth (BMWFJ).

The tariff for new plants may be gradually reduced to reflect the development of costs for a certain technology. The amount of annual reduction is determined by order of the Minister of Economy, Family and Youth, [7].

Entitlement to the tariff is time-limited, regardless of the source of energy used. A given operator of any other renewable energy plant is entitled to the purchase of electricity exported and to the payment of the tariff applicable on the date on which the contract is concluded, for 13 years starting on the date on which the plant is put into operation.

### 3.1.2 Subsidy II (Investment Subsidy for PV)

In addition to the feed-in tariff, an investment subsidy of 30% of the investment costs up to €200 per kW is granted for PV installations on buildings, [8].

Solar energy is eligible under the condition that the installation's capacity exceeds 5 kWp. For PV installations on buildings, the investment subsidy amounts to 30% of the investment costs but no



more than €200 per kWp.

The responsible authority is Ministry of Economy, Family and Youth (BMWFJ)

Until the end of 2014, the support fee is as follows, [7]:

- For users connected to voltage levels 1 to 3: €35,000 per calendar year.
- For users connected to voltage level 4: €35,300 per calendar year.
- For users connected to voltage level 5: €5,200 per calendar year.
- For users connected to voltage level 6: €320 per calendar year.
- For users connected to voltage level 7: €11 per calendar year.

### **3.1.3 Subsidy III (Investment subsidy for small PV)**

Subsidies are granted for PV installations with a maximum capacity of 5kW:

- €275 kWp for roof-top or ground-mounted installations with a maximum capacity of 5 kW.
- €375 kWp for building integrated installations with a maximum capacity of 5 kW.

Subsidies can only be claimed by private parties, [9].

#### **PROCEDURE**

At the beginning of the process, the applicant has to make a request for a registration number. After the number is received, a personal online link to the application form is activated. The construction of the installation has to be accomplished before 15 December 2014. Hereafter, the support form has to be submitted to “Kommunalkredit Public Consulting”. After checking the form and the attached documents, subsidies will be granted. [9]

## 4 COMPARISON OF SUPPORT SCHEMES IN SLOVENIA AND AUSTRIA

This chapter compares the previously described support schemes for both countries. Individual supports cannot be compared, since there are completely different (i.e. loans and premium tariffs in Slovenia-no such support in Austria).

*Table 3: Support schemes in Slovenia and Austria*

AT	SI
<p><b>Feed-in tariff</b></p> <p>Electricity from RES is supported mainly through a feed-in tariff.</p> <p>The operators of RES plants are entitled against the government purchasing agency, the Clearing and Settlement Agency, to the conclusion of a contract on the purchase of the electricity they produce (“obligation to enter into a contract”).</p> <p><b>Subsidy II</b></p> <p>In addition to the feed-in tariff, an investment subsidy is granted for PV installations on buildings exceeding 5 kW.</p> <p><b>Subsidy III</b></p> <p>Furthermore, subsidies are granted for small PV installations with a maximum capacity of 5 kW.</p>	<p><b>Feed-in tariff</b></p> <p>Electricity from RES is supported through a feed-in tariff.</p> <p>Producers of electricity from RES (qualified producers) using plants of up to 1 MW may decide that they would like their electricity to be purchased at a fixed price.</p> <p><b>Premium tariff</b></p> <p>As an alternative, licensed generators may opt for a premium (a so-called “operational subsidy”) on top of the electricity price that they achieve on the free market.</p> <p><b>Subsidies</b></p> <p>In Slovenia, the Ministry of Infrastructure and Spatial Planning (Directorate for Energy, Energy Efficiency and Renewable Energy Sources Division) as well as the Slovenian Environmental Fund (Eko sklad) invite applications for tenders and publish public calls on a regular basis.</p> <p><b>Loans</b></p> <p>The Slovenian Environmental Fund (Eko sklad) invites applications for soft loans.</p>

**Table 4: Comparison of support schemes**

AT	SI
<p><b>Subsidy II (Investment Subsidy for PV)</b></p> <p>For PV installations on buildings, the investment subsidy amounts to 30% of the investment costs but no more than €200 per kW.</p>	<p><b>Subsidy scheme of the Ministry for Infrastructure and Spatial Planning</b></p> <p>The subsidies, state aid and “de minimis” aid are intended to cover some of the costs related to the use of renewable energy instead of traditional energy sources.</p>
<p><b>Subsidy III (Investment subsidy for small PV)</b></p> <p>€275 kWp for roof-top or ground-mounted installations with a maximum capacity of 5 kW.</p> <p>€375 kWp for building integrated installations with a maximum capacity of 5 kW (p. 3PV Guidelines 2014).</p>	<p>Subsidies are subject to a maximum of 50% of the eligible costs of an investment project; state aid and “de minimis” aid grants are subject to a maximum of 30%. Exceptional projects may be awarded 40/50% of the costs. The maximum grant is defined in each specific tender. Certain grants are subject to a maximum (€50,000 for state aid and €200,000 / €100,000 for “de minimis” aid). In these cases, a report must be submitted to the Ministry of Finance.</p>

**Table 5: Comparison of amounts for Feed-in tariff**

Country		Amount	Amount for Solar energy
AT	Feed-in tariff	The amount of tariff is determined for each source of energy by the Minister of Economy, Family and Youth.	<p>PV installations on roof-tops and facades with capacities over 5 kWp, up to 350 kWp, if the application submitted and contract concluded until the end of 2014: €ct 12.5 per kWh.</p> <p>Other PV installations with capacities over 5 kWp, up to 350 kWp, if the application submitted and contract concluded until the end of 2014: €ct 10.00 per kWh.</p>
SI	Feed-in tariff (guaranteed price)	The tariff level mainly depends on the plant size.	<p>The tariff rates are calculated on a monthly basis due to the change in the degression mechanism which implies a monthly degression of the Reference Costs by 2%. The feed-in tariffs for June 2014:</p> <p>Building-mounted PV installations:</p> <ul style="list-style-type: none"> <li>• up to 50 kWp: €ct 10.428 per kWh</li> <li>• up to 1 MWp: €ct 9.536 per kWh</li> <li>• up to 5 MWp: €ct 7.913 per kWh</li> </ul> <p>Other PV installations:</p> <ul style="list-style-type: none"> <li>• up to 50 kWp: €ct 9.798 per kWh</li> <li>• up to 1 MWp: €ct 9.026 per kWh</li> <li>• up to 5 MWp: €ct 7.277 per kWh</li> </ul> <p>Building-mounted PV installations up to 5 kWp which are connected behind the end user's meter are entitled to an additional 5% of the reference costs.</p>

**Table 6: Comparison of Degression for Slovenia and Austria**

Country		Degression
AT	Feed-in tariff	The tariff for new plants may be gradually reduced to reflect the development of costs for a certain technology. The amount of annual reduction is determined by order of the Minister of Economy, Family and Youth.
SI	Feed-in tariff	The tariff rates are calculated on a monthly basis due to the change in the degression mechanism that implies a monthly degression of the Reference Costs by 2%. Building-mounted PV installations up to 5 kWp, which are connected behind the end user's meter are entitled to an additional 5% of the reference costs.

**Table 7: Eligibility period for support in Slovenia and Austria**

Country		Eligibility period
AT	Feed-in tariff	A given operator of any other renewable energy plant is entitled to the purchase of electricity exported and to the payment of the tariff applicable on the date on which the contract is concluded, for <b>13 years</b> starting on the date on which the plant is put into operation.
SI	Feed-in tariff	The uniform annual price is guaranteed for the period agreed on by both contracting parties and laid down in the contract. The price is based on the reference price applicable on the day on which the contract is concluded and will be paid for no more than <b>15 years</b> .

## 5 CONCLUSION

This paper describes energy regulation in the field of solar energy (PV) in Slovenia and Austria. In both countries, the national institutions are the ones who give the subsidies for PV. Slovenia has more types of support compared to Austria. Both countries have feed-in tariffs for which the eligibility period in Slovenia is 15 years and 13 years in Austria. Slovenia has divisions of power plants in three categories: up to 50 kWp, from 50kWp to 1MWp and from 1MWp up to 5MWp. Austria has up to 5 kWp and above 5kWp up to 350kWp. Furthermore, there are differences in amounts.

Slovenia	Austria
Building-mounted PV installations: <ul style="list-style-type: none"> <li>• up to 50 kWp: €ct 10.428 per kWh</li> <li>• up to 1 MWp: €ct 9.536 per kWh</li> <li>• up to 5 MWp: €ct 7.913 per kWh</li> </ul> Other PV installations: <ul style="list-style-type: none"> <li>• up to 50 kWp: €ct 9.798 per kWh</li> <li>• up to 1 MWp: €ct 9.026 per kWh</li> <li>• up to 5 MWp: €ct 7.277 per kWh</li> </ul>	Building-mounted PV installations (on rooftops and facade): <ul style="list-style-type: none"> <li>• from 5kWp up to 350kWp: €ct 12.5 per kWh</li> <li>• up to 1 MWp: €ct 9.536 per kWh</li> </ul> Other PV installations: <ul style="list-style-type: none"> <li>• capacities over 5 kWp, up to 350 kWp: €ct 10.00 per kWh.</li> </ul>

In Slovenia, the generation of electricity from renewable energy sources is supported through a feed-in tariff. Producers of electricity from renewable sources (qualified producers) using plants of up to 1 MW may decide that they would like their electricity to be purchased at a fixed price. In Austria, electricity from renewable sources is supported mainly through a feed-in tariff. The operators of renewable energy plants are entitled against the government purchasing agency to the conclusion of a contract on the purchase of the electricity they produce.

Slovenia has as an alternative for licensed generators. They may opt for a premium (a so-called “operational subsidy”) on top of the electricity price that they achieve on the free market.

In Slovenia, the Ministry of Infrastructure and Spatial Planning (Directorate for Energy, Energy Efficiency and Renewable Energy Sources Division) as well as the Slovenian Environmental Fund (Eko

sklad) invite applications for tenders and publish public calls on a regular basis. The Slovenian Environmental Fund (Eko sklad) also invites applications for soft loans.

In addition to the feed-in tariff, Austria offers an investment subsidy is granted for PV installations on buildings exceeding 5 kW (30% of the investment costs but no more than €200 per kWp) and furthermore, subsidies are granted for small PV installations with a maximum capacity of 5 kW (€275 kWp for roof-top or ground-mounted installations with a maximum capacity of 5 kW and €375 kWp for building integrated installations with a maximum capacity of 5 kW) that can only be claimed by private parties.

## References

- [1] Borzen, organizator trga z električno energijo, d.o.o. ([www.borzen.si/](http://www.borzen.si/))
- [2] *Energy Act - Slovenia* (<http://www.uradni-list.si/1/content?id=116549>)
- [3] *Decree on the Support for Electricity Generated from Renewable Energy Sources, RS 37/2009* (Uredba o podporah električni energiji, proizvedeni iz obnovljivih virov energije – Uradni list RS, 37/2009)
- [4] *Terms and Conditions of the Eco Fund* (Splošni pogoji poslovanja za spodbujanje razvoja na področju varstva okolja – Uradni list RS 117/2005 – General terms and conditions for promoting the development in the field of environmental protection)
- [5] *ZUP* (Zakon o splošnem upravnem postopku - neuradno prečiščeno besedilo, PisRS z dne 22.02.2010 – Administrative Procedures Act)
- [6] *Legal Sources on renewable Energies* (<http://www.res-legal.eu>)
- [7] *ÖSG 2012 - Federal Act on the Support of Electricity Produced from Renewable Energy Sources* (Bundesgesetz, mit dem Neuregelungen auf dem Gebiet der Elektrizitätserzeugung aus Erneuerbaren Energieträgern und auf dem Gebiet der Kraft-Wärme-Kopplung erlassen werden )
- [8] *ÖSET-VO 2012 - Regulation of the Minister of Economy, Family and Youth determining the feed-in tariffs for the purchase of electricity from renewable energy plants on the basis of contracts to whose conclusion the Clearing and Settlement Agency is obligated from 1 July until the end of 2013* (Verordnung des Bundesministers für Wirtschaft, Familie und Jugend, mit der die Einspeisetarife für die Abnahme elektrischer Energie aus Ökostromanlagen auf Grund von Verträgen festgesetzt werden, zu deren Abschluss die Ökostromabwicklungsstelle ab 1. Juli 2012 bis Ende des Jahres 2013 verpflichtet ist)
- [9] *PV Guidelines 2014* (Leitfaden Photovoltaik-Anlagen 2014)

## Nomenclature

<b>PV</b>	Photovoltaics
<b>NEP</b>	National Energy Program
<b>CP</b>	Support Centre
<b>NREAP</b>	National Renewable Energy Action Plan

# NUMERICAL ANALYSIS OF LIFT AND PRESSURE COEFFICIENTS OF AN AIRFOIL: ANSYS VS SOLIDWORKS

## NUMERIČNA ANALIZA KOEFICIENTA VZGONA IN TLAKA PROFILA KRILA: ANSYS IN SOLIDWORKS

Igor Spaseski<sup>✉</sup>, Marko Pezdevšek, Igor Ščuri, Matej Fike, Gorazd Hren

**Keywords:** numerical analysis, airfoil, CFD, Ansys CFX, SolidWorks

### **Abstract**

In this article, curves for the lift and pressure characteristics of an NACA 6508 airfoil at various angles of attack were acquired with numerical simulation software packages: Ansys CFX and SolidWorks Flow Simulation. The analyses were performed using three different mesh resolutions, with similar number of elements, for different angles of attack. Furthermore, all numerically obtained results were compared to the experimental measurements from a reliable source.

### **Povzetek**

V članku so predstavljeni rezultati numerične analize tlačnih koeficientov v okolici profila in koeficienta vzgona pri različnih napadnih kotih za osamljeno krilo s profilom NACA 6508. Za izvedbo numeričnih simulacij sta bila uporabljena programska paketa Ansys CFX ter SolidWorks Flow Simulation. Analiza je bila izvedena s tremi strukturiranimi mrežami različne gostote elementov za več različnih napadnih kotov. Rezultate vseh mrež smo primerjali z eksperimentalno izmerjenimi vrednostmi iz primarne literature.

<sup>✉</sup> Corresponding author: Igor Spaseski, Tel.: +386 31 828 490, Mailing address: Florjanska ulica 125, 8290 Sevnica, Slovenia, E-mail address: [igor.spaseski@gmail.com](mailto:igor.spaseski@gmail.com)

## 1 INTRODUCTION

The evolution of computational fluid dynamics (CFD) is driven by the need for faster and more accurate methods for the calculations of flow fields around configurations of technical interest. For a decade, CFD has been the method of choice in the design of many types of industries and processes in which fluid or gas flows play a significant role. In CFD, there are several commercial packages available for simulating flow in or around objects. The computer simulations show features and details that are difficult, expensive, or impossible to measure or visualize experimentally.

The first step in simulating a problem involves the creation of the geometry (model) and physical model. The majority of the time spent on a CFD project is usually devoted to generating a mesh for the domain geometry that allows a balance between the desired accuracy and solution time. After the creation of the mesh, a solver is able to solve the governing mathematical equations of the problem. Afterwards, the results are validated with experimental measurements, [1].

Many researchers have investigated flow conditions around the isolated profile, experimentally and numerically. In [2] a comparison of flow conditions between an open and closed trailing edge was analysed with Ansys CFX. The flow field around a profile at higher angles of attack was found to be time dependent. Detailed investigation of the flow phenomena requires transient simulations. An investigation of flow conditions around a profile with steady state and transient simulation using Ansys CFX was performed in [3]. The goal of our study is not to numerically investigate the flow field around a profile in detail, but to compare the results of the predicted global parameters such as the lift and pressure coefficients for the two-selected software with experimental results.

## 2 GOAL DEFINITIONS

In order to compare different numerical analysis software, we decided to perform numerical analyses and compare the results to experimental data. The experimental data were obtained from [4] for the lift and pressure characteristics of an airfoil NACA 6508. The comparison was performed at different angles of attack (AOA) from  $0^\circ$  to  $20^\circ$  with  $2^\circ$  step.

Steady-state simulations were made with Ansys CFX 15.0 and SolidWorks Flow Simulation (SWFS) software packages in order to obtain lift and pressure coefficient curves. We have to emphasize the difference of software purpose and limitations. Ansys CFX is well-known commercial standalone numerical software for numerical analyses, and SolidWorks Flow Simulation is part of CAD (Computer-aided design) package.

We attempt to create corresponding meshes and boundary conditions, and to compare the results of analyses, definitions of meshes and user-friendliness of software.

## 3 NUMERICAL MODEL

To obtain reliable results, we created three meshes with different but comparable densities in both numerical packages. SolidWorks Flow Simulation provides only a  $k-\varepsilon$  turbulence model, while Ansys CFX offers more models, so we performed analyses with a  $k-\varepsilon$  turbulence model and the shear stress transport (SST) turbulence model.



### 3.1 Geometry and meshing

2D geometry of NACA 6508 was modelled from [5] in SolidWorks (SW) software and with ICEM CFD 15.0. Furthermore, structural numerical meshes were also designed with this software.

The mesh creation has two primary functions. Firstly, to import characteristic points to model the airfoil and defines the size of the domain; secondly, the discretisation and mesh generation of the computational domain.

Both of the programs used do not allow calculations in 2D; therefore, a 2D numerical mesh was created and extruded into the third dimension for one element of thickness.

The square computational domain around the airfoil was discretised by a structured mesh. The size of the domain was seven lengths of an airfoil chord length ahead of the airfoil and 15 lengths behind the airfoil.

Several simulations of pressure distribution on the airfoil surface were performed to investigate the effect of mesh resolution on the results. Generally, a numerical solution is more accurate with an increased number of elements and nodes with higher densities of elements in areas of interest; consequently, the required computer memory and computational time increases. Therefore, three meshes with different numbers of elements were designed and used for performing simulations at various angles of attack.

In Figures 1 and 2, the parts of structural mesh created in ICEM CFD and SolidWorks are presented, respectively. The resolution of the mesh is greater in regions where greater computational accuracy is needed, such as the region close to the airfoil.

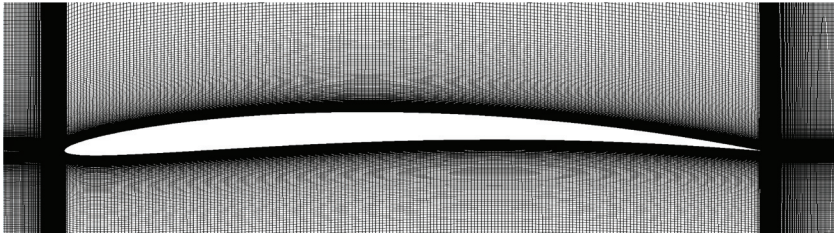


*Figure 1: Numerical mesh designed with ICEM CFD software*

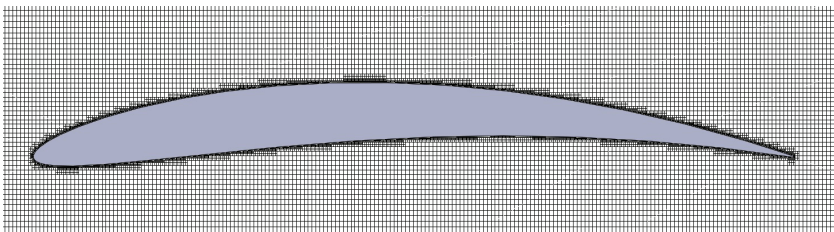


*Figure 2: Numerical mesh designed with SolidWorks software*

In Figure 3, the close-ups of the mesh are shown, which clearly represent a different type of mesh creation. Typical structured mesh from ICEM CFD (a) and the use of a Cartesian-based mesh generation in SolidWorks (b) [6] are presented.

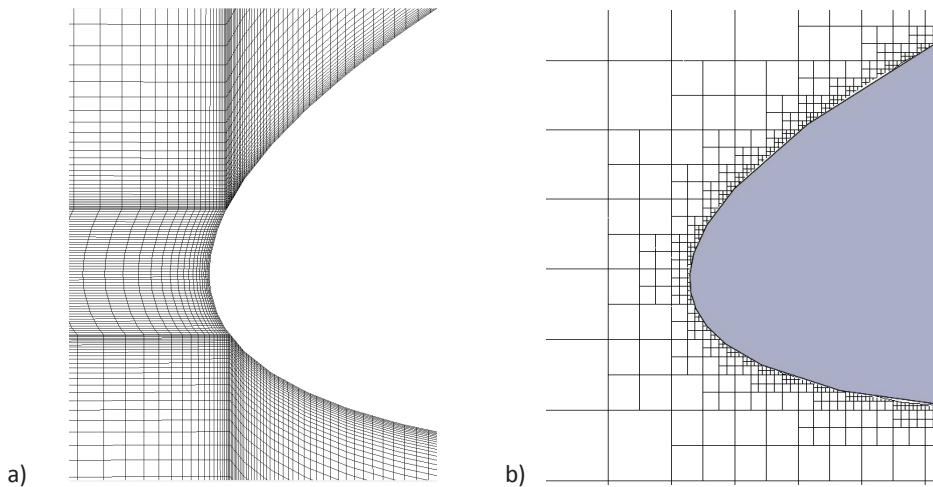


**Figure 3:** Numerical mesh designed with a) ICEM CFD and b) SolidWorks software in close-up view

To investigate the height of the first cell adjacent to the surface of the airfoil, a dimensionless wall distance ( $y^+$ ) simulation was performed. Precise computed results were possible only if the resolution of the mesh near the wall of the airfoil satisfied the condition  $y^+ < 1$ . As seen in Figure 4, the value of  $y^+$  was greater than one only at the nose and the trailing edge of the airfoil.

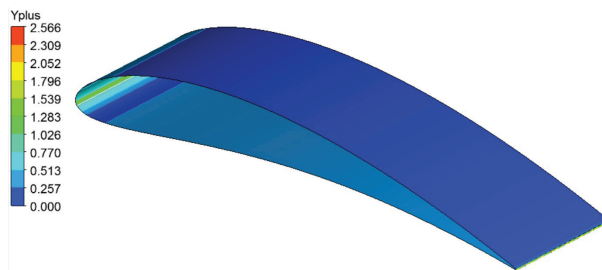


**Figure 4:**  $y^+$  near airfoil wall for the medium mesh at AOA  $10^\circ$

The mesh data of all three meshes are presented in Table 1.

**Table 1: Mesh data**

Mesh resolution	NACA 6508	
	Ansys CFX Number of elements	SolidWorks Number of elements
Coarse	77,940	84,021
Medium	307,980	344,512
Fine	517,044	490,078

### 3.2 Boundary conditions and convergence criteria

The numerical meshes described above were the same for all angles of attack. Therefore, the airfoil was stationary in the domain, and all AOA were defined by changing the inlet velocity vectors. The reference pressure in the domain was set to 100 kPa, and the temperature was 293 K. The following boundary conditions are defined as inlet, opening, wall and symmetry. The left and bottom sides of the domain were defined as inlets (in Ansys CFX). The upper and right side of the domain were defined as openings with a pressure of 100 kPa. For the front and backside, the symmetry boundary condition was used. The airfoil edge was defined as a no-slip wall.

The absolute inlet speed was calculated with equation:

$$v = \frac{Re \cdot \nu}{c}, \quad (3.1)$$

where:

$Re$  - Reynolds number ( $Re=100,000$ );

$\nu$  - kinematic viscosity ( $\nu=15.1 \cdot 10^{-6} \text{ m}^2/\text{s}$ );

$c$  - airfoil chord length.

The calculated speed at inlet was 18.88 m/s, [4]. Components of the velocity vectors  $v_x$  and  $v_y$  for the selected AOA ( $\varphi$ ) were calculated with equations (3.2):

$$\begin{aligned} v_x &= v \cdot \cos \varphi, \\ v_y &= v \cdot \sin \varphi. \end{aligned} \quad (3.2)$$

The air density was set to 1.185 kg/m<sup>3</sup>, the dynamic viscosity to 1.79·10<sup>-5</sup> kg/ms, turbulence intensity to 1.5 % and turbulence length scale to 0.01 m, [4]. To satisfy the convergence criteria, all the RMS leftovers from solving equations must be under 1·10<sup>-5</sup>. We set the number of maximum iterations to 500 and automatic timescale control. For the SST turbulence model at higher AOA, we used a larger physical timescale to ensure convergence. Both software packages have an automatic system for stopping the analysis when it reaches defined convergence criteria.

## 4 RESULTS

The computed results of the pressure distribution on the airfoil surface at different AOA were compared to existing experimental data [4], but there was no data of the lift coefficient, so the lift coefficient results between the two software packages were compared only. Based on the results seen in Figure 7 and the computational times seen in Table 2, we selected the coarse mesh for Ansys *k-ε* and medium mesh for both SolidWorks and Ansys SST.

### 4.1 Pressure distribution on airfoil surface

Pressure is usually presented in the form of a pressure coefficient  $C_p$  and is calculated with the equation:

$$C_p = \frac{p - p_0}{\frac{1}{2} \cdot \rho \cdot v^2}, \quad (4.1)$$

where:

$p$  - simulated (measured) pressure;

$p_0$  - reference pressure (100 kPa);

$\rho$  - air density;

$v$  - airflow speed.

Figures 5 and 6 show the comparison of numerical analysis results and experimental data.

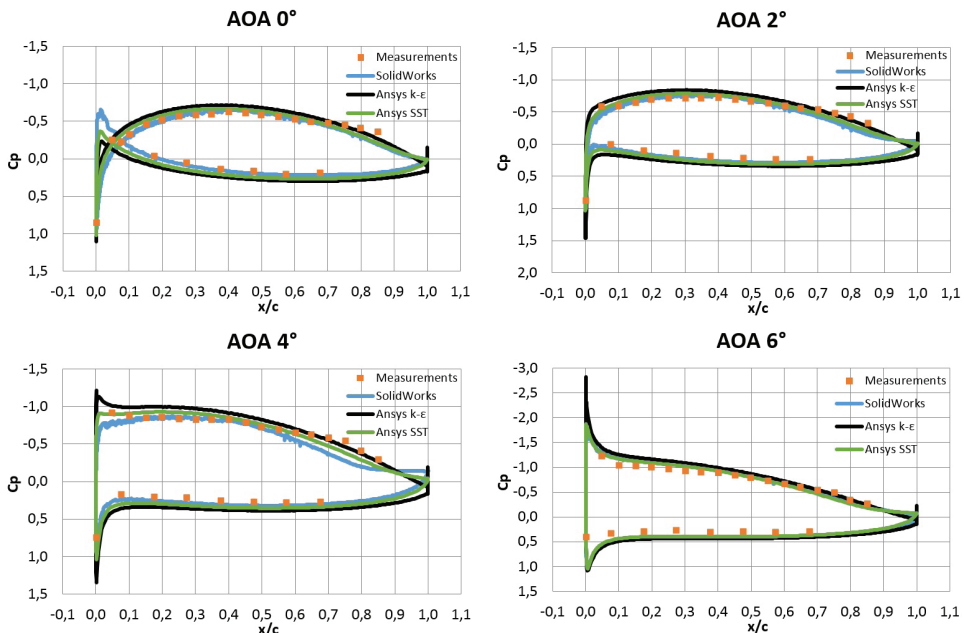


Figure 5: Comparison between experimental and CFD results of  $C_p$  at AOA ranging from  $0^\circ$  to  $6^\circ$

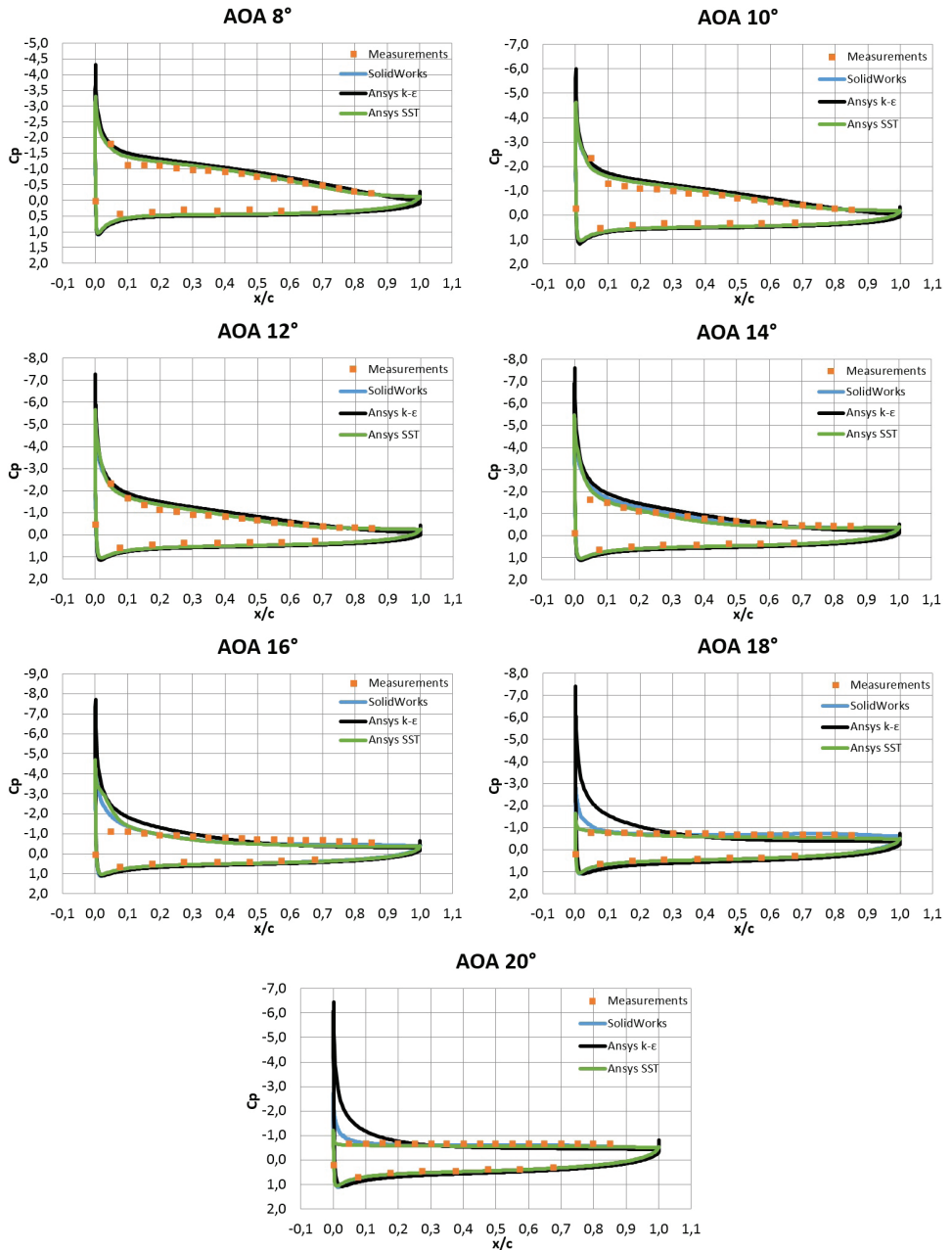


Figure 6: Comparison between experimental and CFD results of  $C_p$  at AOA ranging from 8° to 20°

## 4.2 Lift coefficient

From numerical simulations, we acquired forces in the horizontal and vertical directions from which we calculated the lift force. We calculate the lift coefficient  $C_l$  with the following equation:

$$C_l = \frac{F_l}{\frac{1}{2} \cdot c \cdot \rho \cdot v^2}, \quad (4.2)$$

where:

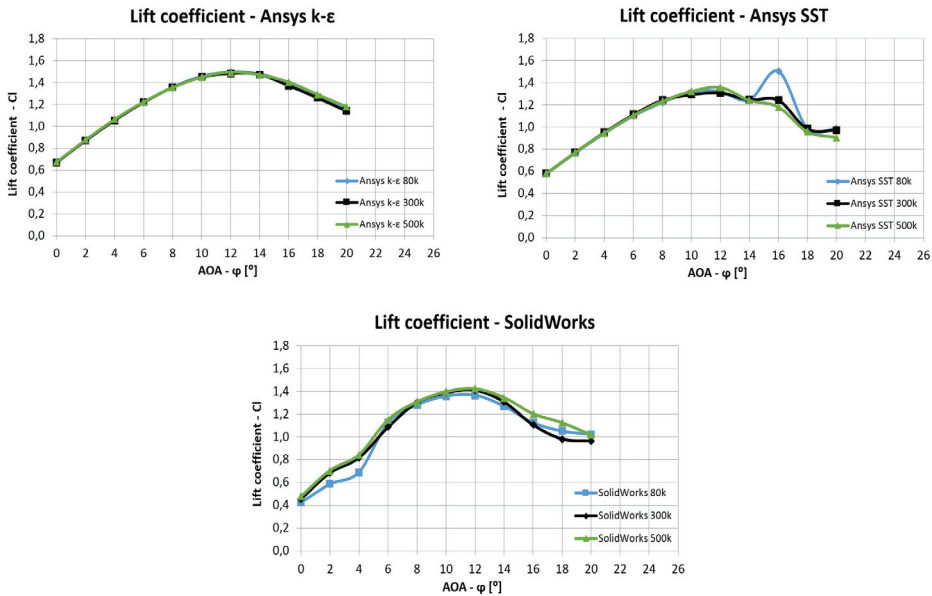
$F_l$  - lift force;

$c$  - airfoil chord length;

$\rho$  - air density;

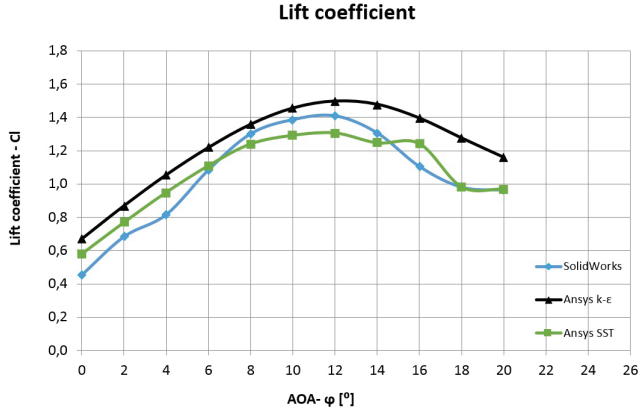
$v$  - air speed.

Figure 7 shows the comparison of numerical analysis for lift coefficient at different AOA with various mesh resolutions.



**Figure 7:** A comparison between numerically obtained values from both software packages of lift coefficients at various AOA for different mesh resolutions

Figure 8 shows the comparison numerically obtained values from both software packages of lift coefficients at various AOA for selected mesh resolution.



**Figure 8:** A comparison between numerically obtained values from both software packages of lift coefficients at various AOA for selected mesh resolution

### 4.3 Computation time

Considering computation times, we present computation times for AOA of 10 ° as a reference. As can be seen in Table 2, computational times in Ansys CFX software using  $k-\epsilon$  turbulence model are longer in comparison to the SST model. Furthermore, the SolidWorks software took about twice as much time to conclude the simulation on a coarse mesh. With increased density of the mesh, the computation time is much longer.

**Table 2:** Computational times for computing pressure distribution on airfoil surface at AOA 10 °

Mesh resolution	Computational time [hh]:[mm]:[ss]		
	Ansys CFX SST model	Ansys CFX $k-\epsilon$ model	SolidWorks
Coarse	0:02:07	0:02:29	0:05:52
Medium	0:07:06	0:10:30	0:45:46
Fine	0:11:13	0:16:01	1:33:30

## 5 CONCLUSIONS

Simulations of pressure distribution on the airfoil surfaces and lift coefficients for various angles of attack were made in order to be able to compare the results from the different software packages and then validate them with existing experimental data from a reliable source.

The difference in accuracy of the results compared to experimental data become more apparent at higher AOA, because the flow on the upper surface of the airfoil begins to separate, and a condition known as stall develops. Different turbulence models predict this effect more or less accurately. Figures 5 and 6 show that the pressure coefficient values computed with Ansys CFX using the  $k-\epsilon$  turbulence model deviates the most from the experimental data. By increasing the angle of attack, this deviation becomes even larger. From the results, we also see that the SST model most accurately describes the pressure coefficient curve. Greater deviation occurred at the angle of  $16^\circ$ , which is the result of the solution not converging; we see this problem with all three meshes. There were no converging problems in the SolidWorks or the  $k-\epsilon$  turbulence model. Results obtained from SolidWorks are quite comparable to experimental data; SolidWorks generally does better than  $k-\epsilon$  but worse than SST in Ansys.

Figure 7 shows how different mesh resolutions affect the lift coefficient curve. With the  $k-\epsilon$  turbulence model, the mesh resolution does not affect results. For the SST model, all the designed meshes were sufficient to the angle of  $10^\circ$ ; at higher angles, the deviation between meshes was larger. The largest deviation occurred at the angle of  $16^\circ$ , which is the angle at which the solution did not converge. We can also see that at this angle the coarse mesh oscillates the most, and its value was about 30 % higher than the fine mesh, while the medium mesh deviated by about 5 %. The medium mesh designed with SolidWorks is sufficient between angles  $0^\circ$  and  $14^\circ$ . At higher AOA, it deviates more and achieves maximum deviation of 15 % at AOA  $18^\circ$ . The coarse mesh in SolidWorks is insufficient at AOA lower than  $6^\circ$  and higher than  $14^\circ$ .

Computational times in Ansys CFX software using  $k-\epsilon$  turbulence model were slightly longer than those using SST model. Furthermore, the SolidWorks software took about twice as much time for performing the simulation on a coarse mesh, as the Ansys SST and  $k-\epsilon$  models did. As the number of elements increases and their size decreases, the computational time in SolidWorks is as much as five times longer than in Ansys CFX. Based on the results seen on Figure 7 and the computational times seen in Table 2, we selected the coarse mesh for Ansys  $k-\epsilon$  and the medium mesh for both SolidWorks and Ansys SST models. The lift coefficient curves of the selected meshes are presented in Figure 8, where we can see that the values of  $k-\epsilon$  model are greater at all AOA. Local maximum of the computed curves was the same at AOA  $12^\circ$ .

Based on the computed results and simulation time, the Ansys SST model has proved to be the most suitable, but if we take into the account the time and effort to make a structured mesh in ICEM CFD, SolidWorks would be the better pick for the example used in this paper.



## References

- [1] **D. C. Eleni, T. I. Athanasios, M. P. Dionissios:** *Evaluation of the turbulence models for the simulation of the flow over a National Advisory Committee for Aeronautics (NACA) 0012 airfoil*, University of Patras - Greece, Department of Mechanical Engineering and Aeronautics, Fluid Mechanics Laboratory (FML), 2012,  
Available at: [http://academicjournals.org/article/article1379753908\\_Eleni\\_et\\_al.pdf](http://academicjournals.org/article/article1379753908_Eleni_et_al.pdf), Accessed on October 6, 2014
- [2] **J. Bitenc, B. Širok, I. Biluš:** *Numerical analysis of flow over a wind turbine airfoil*, Journal of Energy Technology, Volume 6, Issue 4, 2013, pp. 31–46.
- [3] **M. Fike:** *The unsteady static-stall aerodynamic characteristic of an S809 airfoil at low Reynolds numbers*, Journal of Energy Technology, Volume 6, Issue 1, 2013, pp. 33–50.
- [4] **M. Fike:** *Experimental and numerical analysis of fluid flow in an axial fan*, Doctoral thesis, University of Maribor, Faculty of Mechanical Engineering, 2013
- [5] **Airfoil tools:** *NACA 4 digit airfoil generator*,  
Available at: <http://airfoiltools.com/airfoil/naca4digit>, Accessed on October 6, 2014
- [6] **A. Sobachin, G. Dumnov, A. Sobachkin:** *Numerical Basis of CAD-Embedded CFD*, 2014  
Available at: [http://www.solidworks.com/sw/docs/Flow\\_Basis\\_of\\_CAD\\_Embedded\\_CFD\\_Whitepaper.pdf](http://www.solidworks.com/sw/docs/Flow_Basis_of_CAD_Embedded_CFD_Whitepaper.pdf), Accessed on October 6, 2014





# MAIN TITLE OF THE PAPER SLOVENIAN TITLE

*Authors<sup>✉</sup>, Corresponding author*

Keywords: (Up to 10 keywords)

## **Abstract**

Abstract should be up to 500 words long, with no pictures, photos, equations, tables, only text.

## **Povzetek**

(Abstract in Slovenian language)

**Submission of Manuscripts:** All manuscripts must be submitted in English by e-mail to the editorial office at [jet@um.si](mailto:jet@um.si) to ensure fast processing. Instructions for authors are also available online at <http://www.fe.um.si/en/jet/author-instructions.html>.

**Preparation of manuscripts:** Manuscripts must be typed in English in prescribed journal form (MS Word editor). A MS Word template is available at the Journal Home page.

A title page consists of the main title in the English and Slovenian language; the author(s) name(s) as well as the address, affiliation, E-mail address, telephone and fax numbers of author(s). Corresponding author must be indicated.

**Main title:** should be centred and written with capital letters (ARIAL bold 18 pt), in first paragraph in English language, in second paragraph in Slovenian language.

**Key words:** A list of 3 up to 6 key words is essential for indexing purposes. (CALIBRI 10pt)

**Abstract:** Abstract should be up to 500 words long, with no pictures, photos, equations, tables, - text only.

**Povzetek:** - Abstract in Slovenian language.

**Main text** should be structured logically in chapters, sections and sub-sections. Type of letters is Calibri, 10pt, full justified.

---

✉ Corresponding author: Title, Name and Surname, Tel.: +XXX x xxx xxx, Fax: +XXX x xxx xxx, Mailing address: xxx xxxxxxxxxxxxxxxxxxxxxxxxxxxxxxxxx, E-mail address: email@xxx.xx

Units and abbreviations: Required are SI units. Abbreviations must be given in text when first mentioned.

Proofreading: The proof will be send by e-mail to the corresponding author in MS Word's Track changes function. Corresponding author is required to make their proof corrections with accepting or rejecting the tracked changes in document and answer all open comments of proof reader. The corresponding author is responsible to introduce corrections of data in the paper. The Editors are not responsible for damage or loss of submitted text. Contributors are advised to keep copies of their texts, illustrations and all other materials.

The statements, opinions and data contained in this publication are solely those of the individual authors and not of the publisher and the Editors. Neither the publisher nor the Editors can accept any legal responsibility for errors that could appear during the process.

Copyright: Submissions of a publication article implies transfer of the copyright from the author(s) to the publisher upon acceptance of the paper. Accepted papers become the permanent property of "Journal of Energy Technology". All articles published in this journal are protected by copyright, which covers the exclusive rights to reproduce and distribute the article as well as all translation rights. No material can be published without written permission of the publisher.

Chapter examples:

## 1 MAIN CHAPTER

**(Arial bold, 12pt, after paragraph 6pt space)**

### 1.1 Section

**(Arial bold, 11pt, after paragraph 6pt space)**

#### 1.1.1 Sub-section

**(Arial bold, 10pt, after paragraph 6pt space)**

Example of Equation (lined 2 cm from left margin, equation number in normal brackets (section. equation number), lined right margin, paragraph space 6pt before in after line):

$$\text{Equation} \tag{1.1}$$

Tables should have a legend that includes the title of the table at the top of the table. Each table should be cited in the text.

Table legend example:

***Table 1:*** Name of the table (centred, on top of the table)

Figures and images should be labelled sequentially numbered (Arabic numbers) and cited in the text – Fig.1 or Figure 1. The legend should be below the image, picture, photo or drawing.

Figure legend example:

**Figure 1:** *Name of the figure (centred, on bottom of figure, photo, or drawing)*

## **References**

[1] **Name. Surname:** *Title*, Publisher, p.p., Year of Publication

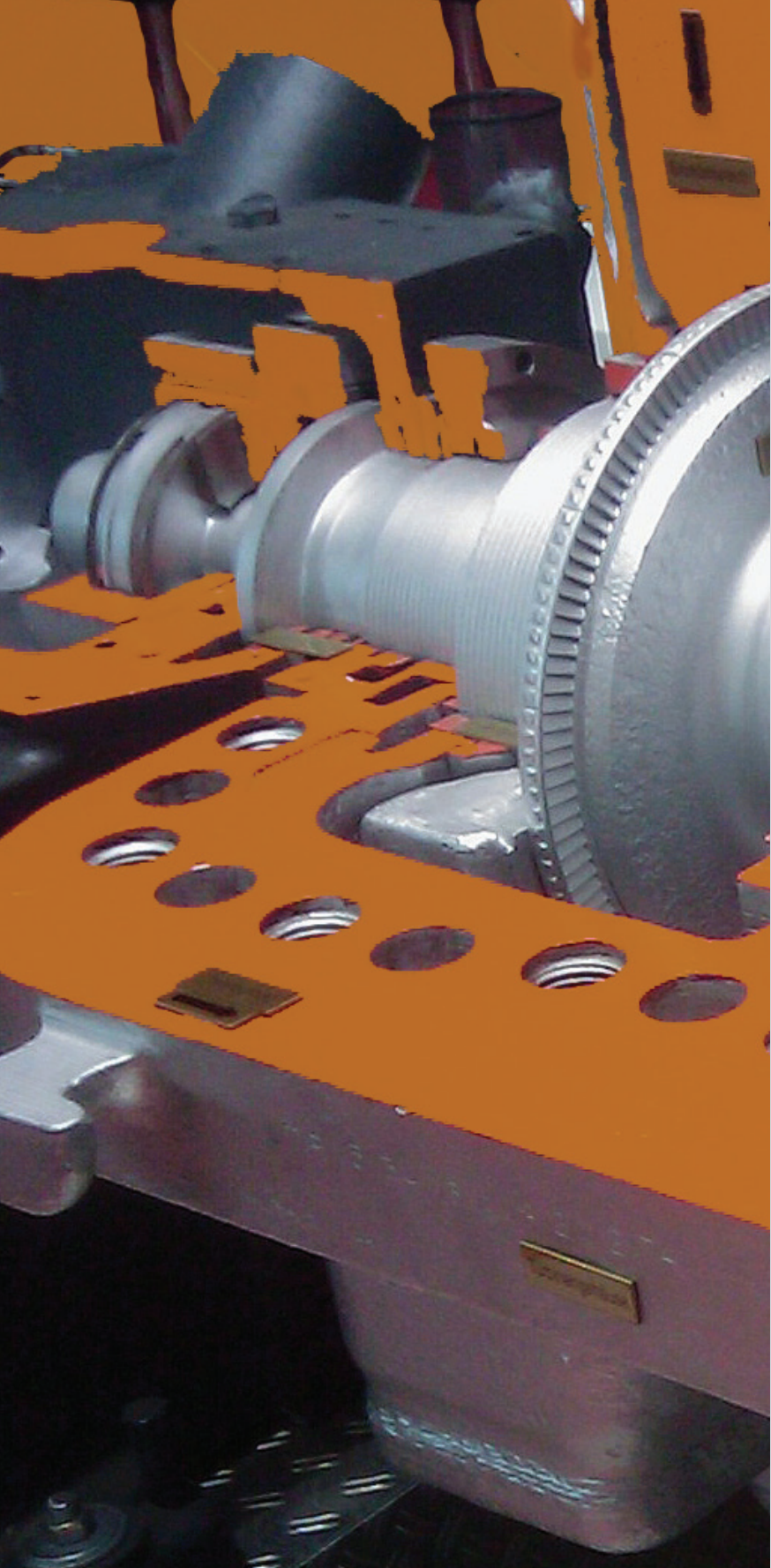
Example of reference-1 citation: In text, *Predin*, [1], text continue. **(Reference number order!)**

## **Nomenclature**

(Symbols)	(Symbol meaning)
<b>t</b>	time







ISSN 1855-5748



9 771855 574008